# CONTROL OF FLASH GAS BYPASS MAC SYSTEM WITH EMPHASIS ON START-UPS AND TRANSIENTS

BY

YUEMING LI

THESIS

Submitted in partial fulfillment of the requirements
for the degree of Master of Science in Mechanical Engineering
in the Graduate College of the
University of Illinois at Urbana-Champaign, 2016

Urbana, Illinois

Advisor:

Professor Predrag S. Hrnjak

# ABSTRACT

Flash Gas Bypass (FGB) approach has the benefits of eliminating refrigerant maldistribution and reducing refrigerant pressure drop across the evaporator. Most of the previous research on flash gas bypass focused on performance improvement in steady state and demonstrated that compared to direct expansion mode (DX), FGB mode have better performance. However, the control strategy of FGB system and dynamic behavior during start-ups and transients were not yet clearly defined and investigated. In this paper, a novel control strategy has been proposed for an automobile air conditioning system operating in flash gas bypass mode with R134a as the refrigerant. This research aims at understanding FGB system performance in dynamic and transient load conditions using Sporlan electronic flow controls.

This research identified three important issues for FGB system start-up process: size of bypass valve, size of FGB tank and control strategy for system operation. Although the exact sizing of both valve and FGB tank would be different from system to system, this study gave a basic guideline and a practical example of choosing corresponding components. More importantly, an innovative control strategy was implemented to make sure FGB system could be well-functioned under different working conditions in both start-up and transient scenarios automatically.

The proposed control strategy utilized an electronic expansion valve (EV) for the control of subcooling from condenser outlet and a bypass valve(BV) for superheat from compressor inlet. Both start-up and transient system behaviors were studied. Transients include changes in air mass flow rate on evaporator side, face velocity on condenser side and compressor speed. The experimental results showed that the proposed cycle control strategy was found to be able to provide reliable control to the system.

*To my parents*

# ACKNOWLEDGMENTS

I would like to first and foremost express my greatest gratitude to my advisor, Professor Pega Hrnjak, whose constant intelligence and tremendous support always gave me the courage to be focused and dedicated to my work. His encouragement and bigger picture about research kept me moving whenever I met with problems.

I am also greatly thankful for the support provided by Dave Wrocklage, Raghu Kunapuli, and all other representatives at Parker Hannifin. Their generous financial assistance and technical help make this project possible and successful. Hope this collaboration will become more and more successful in the following years.

I would also like to thank to my colleagues Dr. Neal Lawrence, Huize Li, Lili Feng, Jiu Xu, Shenghan Jin, Jun Li, Houpei Li, Wenzhe Li, Yu Kang, Lin Zhu, and so many others in ACRC for the valuable discussion and help they provided for experimental facility building and operation. I would also like to express my sincerely thanks to Dejan Beatovic; without his help with building the facility, the project couldn't be finished.

Thanks also go to my boyfriend Xiao Chen and all my other friends beyond research. They gave me the lifelong memory of happiness and joyfulness during these two years.

At last, I would like to thank my parents for their love. They are always there for me even at the most difficult time. Their support is the driving force to make me stronger.

# TABLE OF CONTENTS

# LIST OF FIGURES

# LIST OF TABLES

# NOMENCLATURE

| | | |
|---|---|---|
| **BV** | bypass valve | |
| **COP** | coefficient of performance | |
| **DTsc** | subcooling | (ºC) |
| **DTsh** | superheat | (ºC) |
| **DX** | direct expansion | (ºC) |
| **EV** | electric expansion valve | |
| **FGB** | flash gas bypass | |
| **HX** | heat exchanger | |
| **h** | refrigerant enthalpy | ($kJ \cdot kg^{-1}$) |
| **IHX** | internal heat exchanger | ($kJ \cdot kg^{-1}$) |
| $\dot{m}$ | mass flow rate | ($g \cdot s^{-1}$) |
| **MAC** | automobile air conditioning | |
| **MCHX** | microchannel heat exchanger | |
| **P** | pressure | (kPa) |
| **PID** | proportional integral derivative | |
| **Q** | cooling capacity | (kW) |
| **t** | time | (s) |
| **T** | temperature | (ºC) |
| $\mathbf{V_C}$ | compressor speed | (rpm) |
| $\mathbf{W_C}$ | compressor power | (kW) |
| **x** | refrigerant quality | |

## Subscripts

| | |
|---|---|
| **a** | air side |
| **c** | condenser |
| **cai** | condenser air inlet |
| **cao** | condenser air outlet |
| **cpri** | compressor refrigerant inlet |
| **cpro** | compressor refrigerant outlet |
| **cri** | condenser refrigerant inlet |
| **cro** | condenser refrigerant outlet |
| **e** | evaporator |
| **eai** | evaporator air inlet |
| **eao** | evaporator air outlet |
| **eri** | evaporator refrigerant inlet |
| **ero** | evaporator refrigerant outlet |
| **ihxrli** | internal heat exchanger low-pressure side inlet |
| **i** | inlet |
| **en** | indoor nozzle |
| **o** | outlet |
| **r** | refrigerant side |
| **xri** | expansion valve refrigerant inlet |
| **xro** | expansion valve refrigerant outlet |

# CHAPTER 1 INTRODUCTION

## 1.1 Background

### 1.1.1 Flash gas bypass

Nowadays, microchannel heat exchangers (MCHX) are widely used in many applications, especially in evaporators and condensers for automobile air conditioning (MAC) systems. The main advantages for MCHX can be summarized as higher overall heat transfer coefficient, lower refrigerant inventory, more compactness, lower cost and weight. However, the parallel flow structure of MCHX will cause non-uniform distribution, also called maldistribution since it is difficult to feed same quantity of refrigerant to each microchannel tube. The problem is more serious for evaporator because maldistribution will result in poor utilization of heat transfer area, thus decreased the cooling capacity. There was numerous research in the last decade on how to quantify refrigerant maldistribution (Vist and Pettersen, 2004; Kim and Kim, 2011; Zou and Hrnjak, 2013; Li and Hrnjak, 2015a) and its effect on cooling capacity (Kulkarni et al., 2004; Zou et al., 2014; Li and Hrnjak, 2015b).

To improve refrigerant distribution in MCHX, many attempts have been made by a lot of scholars in many open literatures. One solution to this problem is flash gas bypass (FGB) approach, which feeds only liquid to microchannel evaporators and bypasses the vapor refrigerant since vapor is the main reason to cause maldistribution among parallel tubes and it has very small impact on cooling capacity. The FGB concept was first proposed and validated by Beaver et. Al (1999) and it was demonstrated that COP increased up to 20%

by keeping the same capacity of an R744 residential A/C system compared to direct expansion. Later, Elbel and Hrnjak (2004) implemented FGB concept into transcritical R744 system and identified three detailed benefits: 1) reducing the refrigerant-side pressure drop of microchannel evaporator; 2) increasing the refrigerant-side heat transfer coefficient; 3) improving the refrigerant distribution in the evaporator inlet header. Most recently, Tuo and Hrnjak (2012) reported significant improvement of capacity and COP in automobile A/C systems using flash gas bypass.

Same authors (2013) reported periodic reverse flow in a FGB system. Periodic oscillation of pressure at the evaporator inlet was discovered. Through visualization of the flow regime in the inlet header, they divided one oscillation cycle into three parts: 1) reverse vapor flow; 2) vapor re-entraining in forward flow; 3) liquid refilling in forward flow. The vapor re-entraining significantly deteriorated the refrigerant distribution. Tuo and Hrnjak (2014) and Li and Hrnjak (2016) visualized the flow regime in an electrically heated glass channel and an air heated aluminum channel, respectively. Both of them confirmed the existence of flow reversal within microchannel heat exchangers. A theoretical model, which demonstrates the mechanism of flow reversal can be found in Li and Hrnjak (2017).

The previous work demonstrated good potential for improvement of system performance using flash gas bypass concept. However, all the studies were conducted at steady state with manual flow control and very limited work have been done to understand FGB system performance in dynamic and transient working load conditions.

### 1.1.2 Subcooling control

Apart from flash gas bypass, subcooling control has been proven to be another way to improve the performance of vapor compression system. Pottker and Hrnjak (2015) demonstrated that COP has a maximum as condenser subcooling increases due to a trade-off effect by using cycle analysis and modeling of an air conditioning system. As shown in Figure 1-1, refrigerating effect (by $\Delta q$) increases since the refrigerant temperature from condenser outlet decreases (by $\Delta T_{c,out}$), while specific compression work (by $\Delta w$) also increases due to the increase in condensing pressure (by $\Delta T_{c,\mathrm{sat}}$). These two effects compete, and the so-called COP maximizing subcooling exists. The experimental results provided by Pottker and Hrnjak (2015) showed the same conclusion that COP undergoes a maximum as an effect of condenser subcooling. They also showed that even though internal heat exchanger (IHX) would reduce the COP increase by condenser subcooling, the overall efficiency of the system would still go higher. At a given condition, the system COP increased up to 9% for R134a by finding the optimal subcooling.

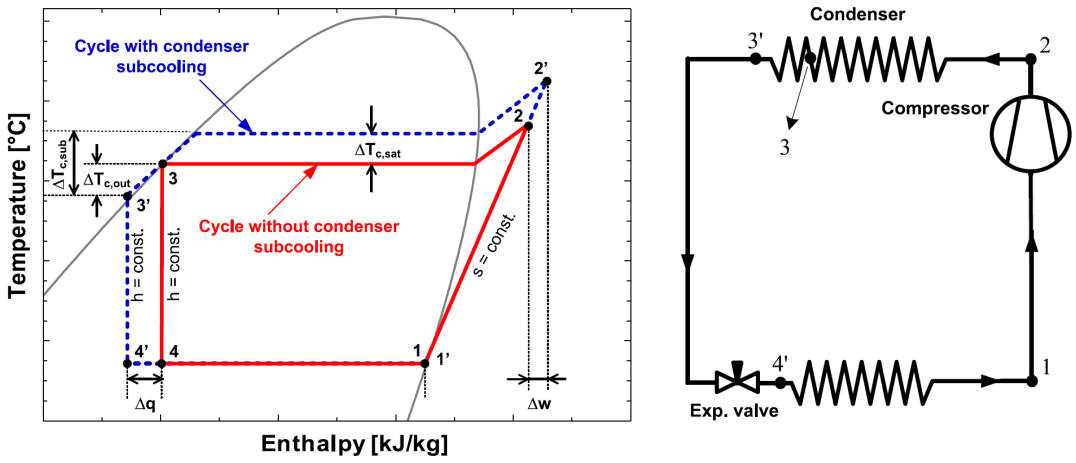


Figure 1-1 Comparison between theoretical cycles with and without condenser subcooling (Pottker and Hrnjak, 2015)

Xu and Hrnjak (2014) continued the work, and they expanded the subcooling study to the residential air-conditioning system with both numerical and experimental investigations and they found that under a specified condition, the maximum COP improvement achieved was up to 33% and the maximum cooling capacity gain is 14.7%. Both simulation and experimental results indicated that the COP maximizing subcooling would increase with ambient temperature (Tcai) increases.

## 1.2 Objective

Based on the previous study, it has been demonstrated that both flash gas bypass and subcooling control could improve system performance. However, few study focus on investigating applicable control strategy and understanding system performance under dynamic and transient working conditions. In flash gas bypass system, it is crucial to maintain a certain liquid level inside FGB tank and make sure only liquid is fed into evaporator which requires proper sizing of FGB tank as well as functional control strategy. At the same time, to prevent liquid from flooding into compressor during start-ups, a reliable and effective control strategy is crucial to the industrial application of flash gas bypass system.

This study aims to combine the benefits of flash gas bypass and subcooling control in automobile air conditioning system and focus on understanding system performance under dynamic and transient working conditions. The performance under start-ups and transients such as changes in compressor speed, air flow rate through evaporator and condenser will be studied, and an appropriate control strategy to avoid flooded compressor and maintain

system robustness will be proposed. In addition, proper sizing of bypass valve and FGB tank have also be studied.

# CHAPTER 2 EXPERIMENTAL SETUP

## 2.1 Test facility and instrumentation

The experimental facility used in this study is shown in Figure 2-1, including refrigeration circuit and an environmental chamber which has been partitioned to be one indoor chamber and one outdoor chamber. In each chamber, heat exchangers are installed at the inlet of an open-loop wind tunnel and electrical heaters were used to control the air inlet temperature to the heat exchangers. Both chambers have a secondary refrigerant cycle with evaporator coil and a condensing unit which can help remove the heat rejected by the condenser, electrical fans, and blowers. Air flow rate through the evaporator is controlled with variable speed blowers. Air-side pressure across the nozzle measuring by pressure differential transducer and dry-bulb air temperature by Type-T thermocouple are used to calculate the actual air flow rates. Within the inlet and outlet of the heat exchangers, thermocouple grids measure the temperature of the inlet and outlet air, respectively. Outside of the environmental chamber, an automobile compressor, an internal heat exchanger (IHX) and a flash gas bypass tank are placed in a frame for easier operation and monitor.

The refrigerant loop consists of a variable speed compressor, a microchannel evaporator, a microchannel condenser, an internal heat exchanger and two electrical valves, including expansion valve (EV) and bypass valve (BV). The integrated receiver has been taken out, and it gives us the possibility to use the so-called flash gas bypass (FGB) tank or separator instead. After the 2500-step electronic expansion device, two-phase refrigerant enters the middle part of flash gas bypass tank; only liquid refrigerant is fed into evaporator

while vapor refrigerant is bypassed though electronic bypass valve. Then two streams of refrigerant join into one stream and then go through internal heat exchanger into the compressor. The condenser used in this study is a 3-pass condenser with 33 tubes, while the original six-pass and two-slab evaporator has been replaced by the one with single-pass and single-slab design for better distribution in the inlet header achieved by FGB. The compressor used in the experimental study is a variable speed compressor with a displacement of 90 $cm^3$, and the speed can be controlled by a variable frequency driver (VFD). It should be noted that the expansion device used in this study is an electronic expansion valve which has 2500 steps, while the bypass valve is also an electronic flow regulating valve which also has 2500 steps. These two valves give us the possibility and freedom to control the system subcooling and superheat, thus controlling the whole system during start-ups and transients.

The uncertainty for measured variables is presented in Table 2-1.

Table 2-1 Measured uncertainties

| **Measurement** | **Unit** | **Uncertainty** |
|---|---|---|
| Refrigerant pressure | kPa | ±3.56 |
| Nozzle pressure drop | Pa | ±6.5 |
| Temperature | °C | ±0.5 |
| Refrigerant mass flow rate | - | ±0.5% |
| Compressor speed | rpm | ±5 |

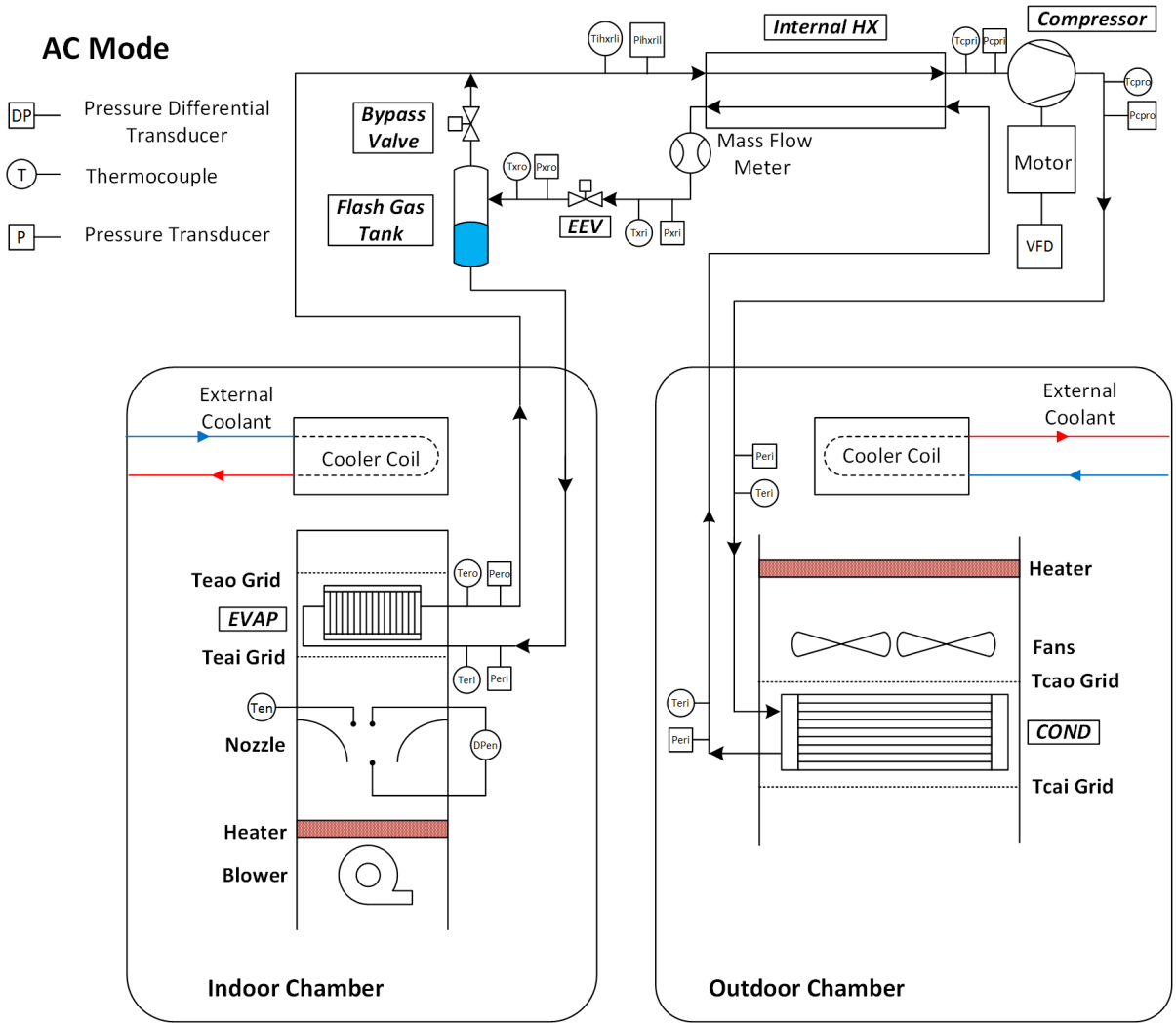


Figure 2-1 Schematic of test facility for flash gas bypass system in air conditioning mode

The efficiency and compactness of the flash gas bypass tank are crucial to the implementation of FGB into real automobile air conditioning system. The flash gas bypass tank is a vertical T-junction separator which is first introduced by Milosevic and Hrnjak (2010) and after thoroughly studied by Tuo and Hrnjak (2014) concerning the effects of geometry under a wide range of operating conditions. The two-phase refrigerant after the expansion device will enter the FGB tank in the middle part of the T junction and then separated into liquid phase and vapor phase. The liquid phase will come out from the

bottom and go into the evaporator while the vapor phase will come out from the upper side and then regulate by BV. The whole tank is made to be transparent so the liquid level inside can be easily monitored.

## 2.2 Control strategy analysis

As shown in Figure 2-2, instead of high-pressure receiver or accumulator, the excessive refrigerant is stored in the so-called separator or FGB tank. This configuration allows throttling to be achieved by fixed area expansion such as orifices, capillary tube and valve.

In this system, a stepper motor valve with 2500 steps has been used as expansion valve. By controlling the opening of the expansion valve, we can control the subcooling of condenser outlet. That control of subcooling can provide additional improvements in efficiency and capacity as elaborated in Chapter 1. For safety operation of the compressor, superheat of the compressor inlet should be maintained by controlling bypass flow using bypass valve, which is also a stepper motor valve with 2500 steps. Two PID controllers are used to maintain desired values for subcooling and superheat.

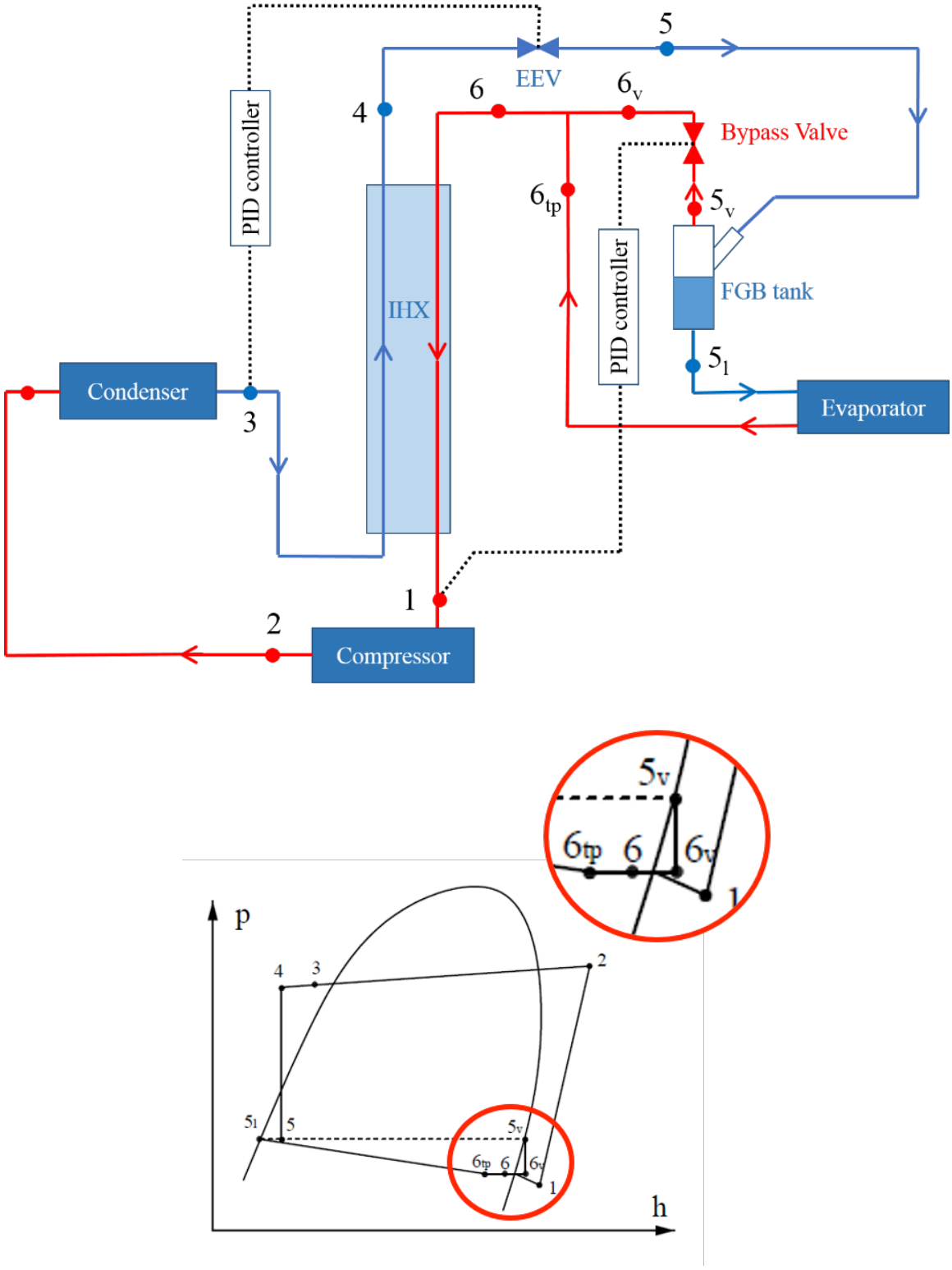


Figure 2-2 System configuration and refrigerant cycle in P-h diagram for FGB system

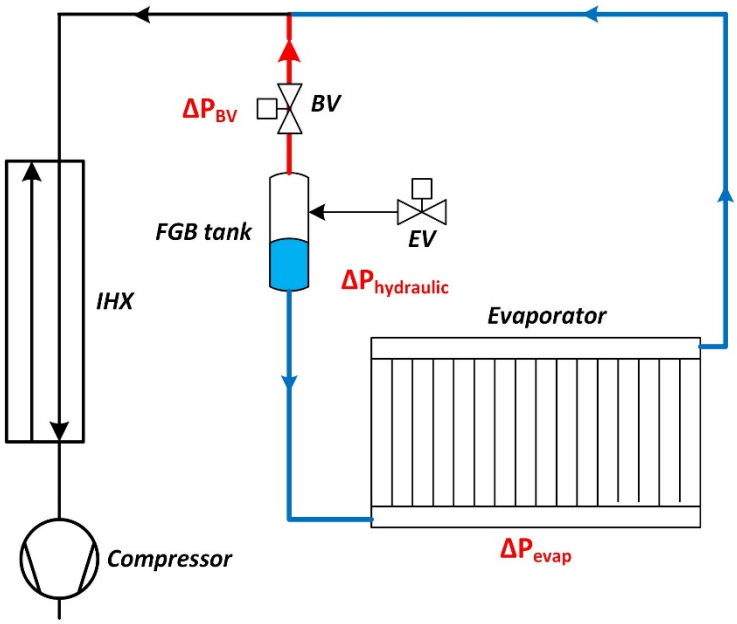


Figure 2-3 Simplified schematic of FGB system

With EV opening going up, the pressure drop across the expansion device goes down, causing condensing pressure going down thus making subcooling smaller. If the in-time subcooling is higher than the desired value, EV will be opened more automatically by PID controller.

As for the relationship among BV opening, superheat and liquid level in FGB tank, it could be summarized that higher BV opening, the higher liquid level and the higher superheat will be. As shown in Figure 2-3 and Equation (2-1), the pressure drop across the bypass valve ($\Delta P_{BV}$) equals to the pressure drop across the microchannel evaporator($\Delta P_{evap}$) minus hydraulic pressure of the excessive refrigerant stored in FGB tank ($\Delta P_{hydraulic}$). When the BV opening is higher, $\Delta P_{BV}$ will be smaller, and then the hydraulic pressure will go up to balance the difference. Since the hydraulic pressure is directly proportional to the liquid level, liquid level will go up under this circumstance. In consequence, more liquid

tend to stay in the FGB tank will result in less refrigerant in evaporator thus causing the superheat going up.

$$\Delta P_{BV} = \Delta P_{evap} - \Delta P_{hydraulic} \quad (2\text{-}1)$$

Therefore, if the in-time superheat is too low, BV will be opened more automatically so both superheat and liquid level in FGB tank will be higher.

Even though the principle of how to take use of EV and BV to control subcooling and superheat is simple, it might have some other issues in practical. One reason is the system is a multiple-input and multiple-output (MIMO) system, changing one of EV and BV will cause both subcooling and superheat change accordingly. To solve it, proper sets of PID parameters for subcooling and superheat controller need to be studied and tuned, which will be elaborated in details in Chapter 4. On the other hand, the special algorithm of BV and superheat will cause flooded compressor even worse if not well-controlled at the start-ups, especially when liquid level is continuously going higher which will cause liquid coming into the compressor immediately without evaporation due to the continuous opening of BV per to the PID controller as elaborated in Chapter 3. These problems should be taken into consideration and a thoroughly, well-functioned control strategy is needed.

# CHAPTER 3 PROPER SIZING OF FGB TANK AND CONTROL STRATEGY TO AVOID LIQUID IN COMPRESSION SUCTION AT START-UPS

## 3.1 Acceptance Criteria

During start-ups of MAC system, compressor reliability is the most important factor and the biggest concern. Once compressor starts working, the pressure difference across the suction and discharge line will cause refrigerant in the evaporator moving towards compressor. There are two ways that liquid could possibly come to the compressor: one is through bypass valve and the another one is through evaporator. To prevent flooding compressor, the liquid level in FGB tank shouldn't be too high during start-ups, which requires good control strategy and proper size of bypass valve. On the other hand, the size of FGB tank should also be well designed to store the excessive refrigerant and avoid flooding of the flash tank, in particular for lower working load where active charge is less.

In this chapter, we will first investigate and choose a proper size of bypass valve. Two Sporlan electric pressure-regulating CDS series valve type were used in this experiment. Later we will decide a proper size of FGB tank by tests under different working loads and record the corresponding liquid level. A proper size of FGB tank will make sure liquid level is maintained at a certain level for different ambient temperatures ranging from 25°C to 40°C. At the end of this chapter, control strategy with different initial BV openings is discussed by start-up experimental results.

## 3.2 Size of bypass valve

A proper size of bypass valve is a crucial factor for superheat control and it should be well-chosen to regulate the bypass vapor properly. Two different sizes of bypass valve are compared under working conditions as shown in Table 3-1. To quantify the efficiency of allowing fluid flow through the valve, the flow factor of the valve, which is also denoted as $C_v$ value is given. It describes the relationship between pressure drop across the valve at a corresponding flow rate. The flow factors for the two bypass valves in this experiment are 1.36 and 2.97, respectively.

The PID parameters are shown in Table 3-2. P value for a bigger bypass valve ($C_v$ = 2.97) is smaller than the valve with smaller $C_v$ since its opening for one step of motor is higher.

Table 3-1 Test conditions for bypass valve sizing

| Compressor Speed (rpm) | Condenser | | Evaporator | |
|---|---|---|---|---|
| | Temp (°C) | Face Velocity(m/s) | Temp (°C) | Mass Flow (kg/min) |
| 900 | 25 | 1.5 | 25 | 9 |

Table 3-2 PID parameters for bypass valve sizing

| | **P** | **I** | **D** |
|---|---|---|---|
| Subcooling control | 0.3 | 0 | 0.1 |
| Superheat control for $C_v$=2.97 | 0.05 | 0 | 0 |
| Superheat control for $C_v$=1.36 | 0.1 | 0 | 0 |

As shown in Figure 3-1 and Figure 3-2, subcooling will be well-controlled by expansion valve which demonstrates that EV is well-chosen in this case. However, for

superheat control shown in Figure 3-3, even the valve with $C_v$ = 1.36 is fully open after 6 mins, the superheat is still lower than target, indicating restriction of the smaller valve while bigger valve with $C_v$ = 2.97 obviously is a better choice to maintain superheat near target value.

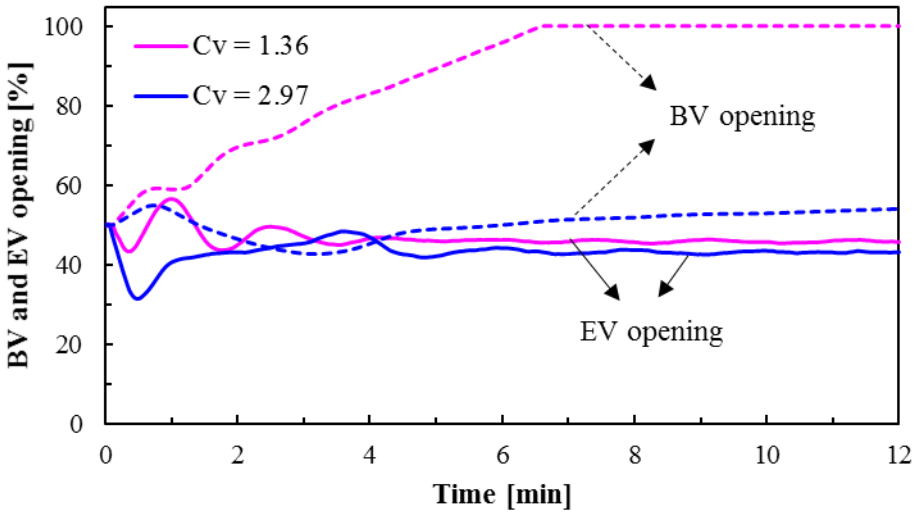


Figure 3-1 EV and BV opening using different BV sizing during start-ups

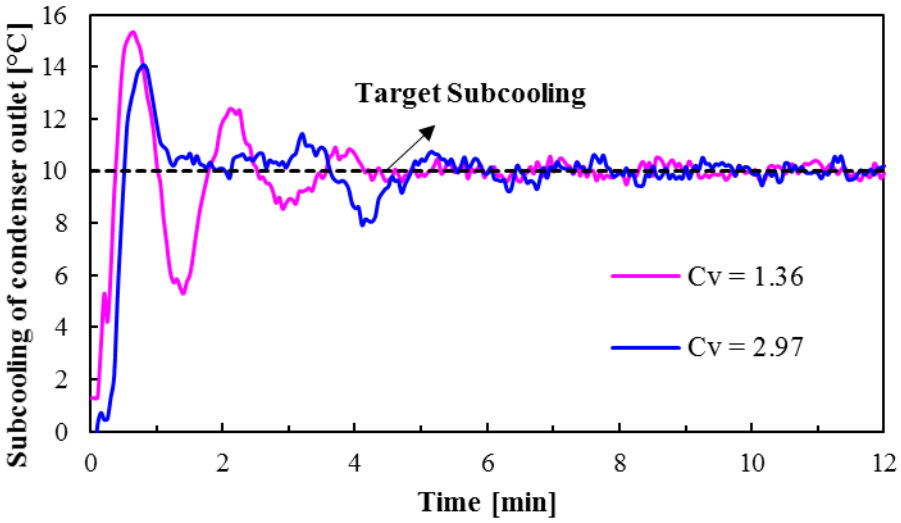


Figure 3-2 Subcooling of condenser outlet variation using different BV sizing

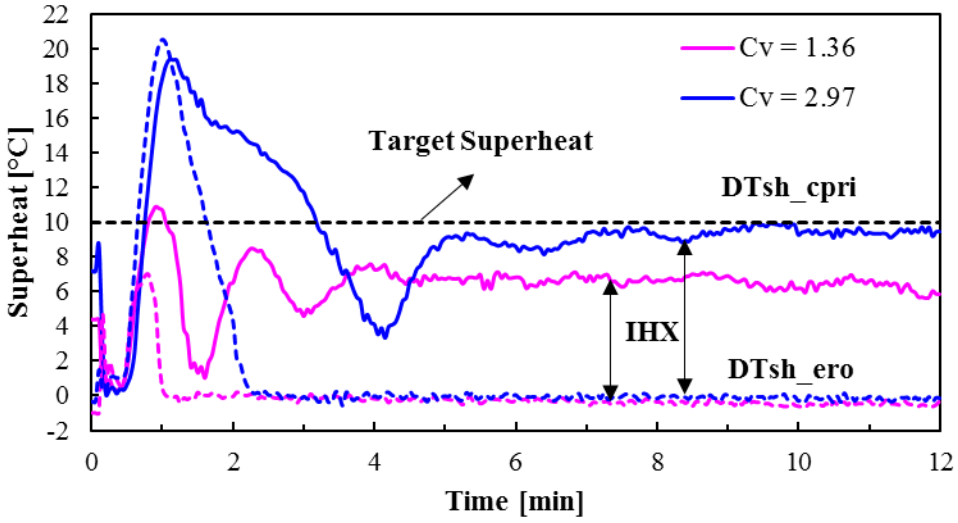


Figure 3-3 Superheat variation using different BV sizing

To ensure superheat of compressor inlet, bypass valve with $C_v = 2.97$ is chosen for later investigations in this study since it has a better performance than the valve with $C_v = 1.36$.

## 3.3 Size of FGB tank

Apart from sizing of bypass valve, the size of FGB tank is also of great importance to maintain a certain liquid level under different working loads. If the liquid level is too low, vapor might be fed into evaporator thus decreasing the performance of the system. However, if the liquid level is too high, separation efficiency would decrease. Moreover, there is a chance that liquid will flood into the compressor through bypass valve, which will harm the compressor. In this experiments, a proper liquid level should be recognizable and lower than the junction point where two-phase refrigerant comes into the tank.

To study the proper size of FGB tank, four tests with different chamber temperatures are compared and the tests conditions are shown in Table 3-3. As Tuo and Hrnjak (2012) reported that the optimal refrigerant charge of flash gas bypass system is higher than direct

expansion system which feeds two-phase refrigerant directly into evaporator and the charge difference is mainly due to the existence of flash gas bypass tank. On the other hand, using the FGB tank will lead to the removal of high side receiver so the refrigerant charge might not be necessarily higher in real applications. However, for different ambient temperatures, the liquid level in the FGB tank should be different due to different working loads. Theoretically, the higher ambient temperature is, higher working load and more refrigerant is needed in evaporator, which causes the liquid level drops down.

By increasing the ambient temperature from 25°C to 40°C, the liquid level for each test case is recorded in Figure 3-4. The other parameters such as compressor speed, condenser face velocity and evaporator mass flow rate are kept the same. Following the results by Xu and Hrnjak (2014), as the ambient temperature goes higher, the COP optimizing subcooling will also be higher ranging from 10 to 13°. Superheat of the system is set to be 10°C to avoid flooded compressor.

Table 3-3 Test conditions for different working loads

| Test Case | Compressor Speed [rpm] | Condenser | | Evaporator | | Set Subcooling [°C] | Set Superheat [°C] | Charge [g] |
|---|---|---|---|---|---|---|---|---|
| | | Temp [°C] | Face Velocity[m/s] | Temp [°C] | Mass Flow [kg/min] | | | |
| A | 900 | 25 | 1.5 | 25 | 9 | 10 | 10 | 1450 |
| B | 900 | 30 | 1.5 | 30 | 9 | 11 | 10 | 1450 |
| C | 900 | 35 | 1.5 | 35 | 9 | 12 | 10 | 1487 |
| D | 900 | 40 | 1.5 | 40 | 9 | 13 | 10 | 1487 |

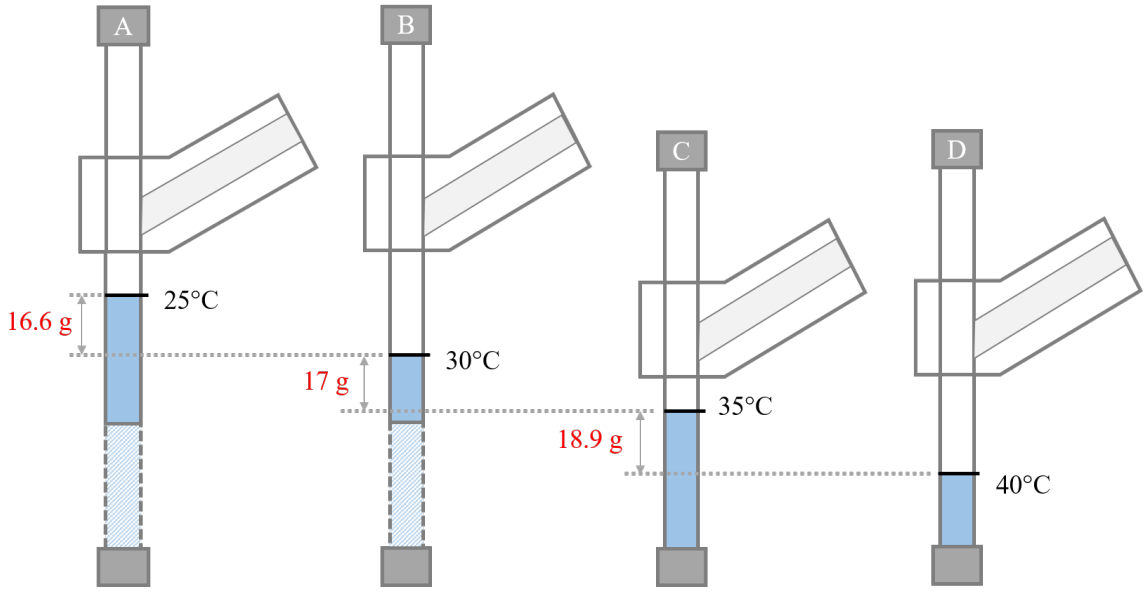


Figure 3-4 Liquid level in FGB tank and charge imbalance for different ambient temperatures
Ambient temperature: A) 25°C; B) 30°C; C) 35°C; D) 40°C

It can be easily noted that with the ambient temperature goes higher, liquid level will also be higher and the charge imbalance between each adjacent test case is around 16.6 to 18.9 grams. The total refrigerant charge for case A and B is 1450 grams while 1487 grams of refrigerant is charged for case C and D to overcome the existing design of FGB tank which is shown in C and D. A more appropriate FGB tank should have bigger room after the seperation juction. By roughly calculation, the new FGB tank have to store at least 80 grams R134a, which is 63 $cm^3$ accordingly.

## 3.4 Effect of initial bypass valve opening

Flooded start is one of most common compressor failure reason in real applications. To avoid flooded compressor during start-ups for FGB system, control strategy is investigated in details. As described above, to avoid liquid coming into the compressor during start-ups, the bypass valve should be operating at a reasonable opening. If the bypass valve opening

is too big, liquid level in FGB tank can easily go too high and then liquid refrigerant will easily come into the IHX. More often, compressor will be flooded since IHX couldn't evaporate all liquid. On the other hand, if the initial bypass valve opening is too small during the start-up, all liquid would come into evaporator making the superheat decrease a lot. A balance and trade-off concerning initial bypass valve opening is the key to ensuring the safety operation.

Table 3-4 Test conditions for initial BV opening study

| Compressor Speed (rpm) | Condenser | | Evaporator | |
|---|---|---|---|---|
| | Temp (°C) | Face Velocity(m/s) | Temp (°C) | Mass Flow (kg/min) |
| 900 | 35 | 1.5 | 35 | 9 |

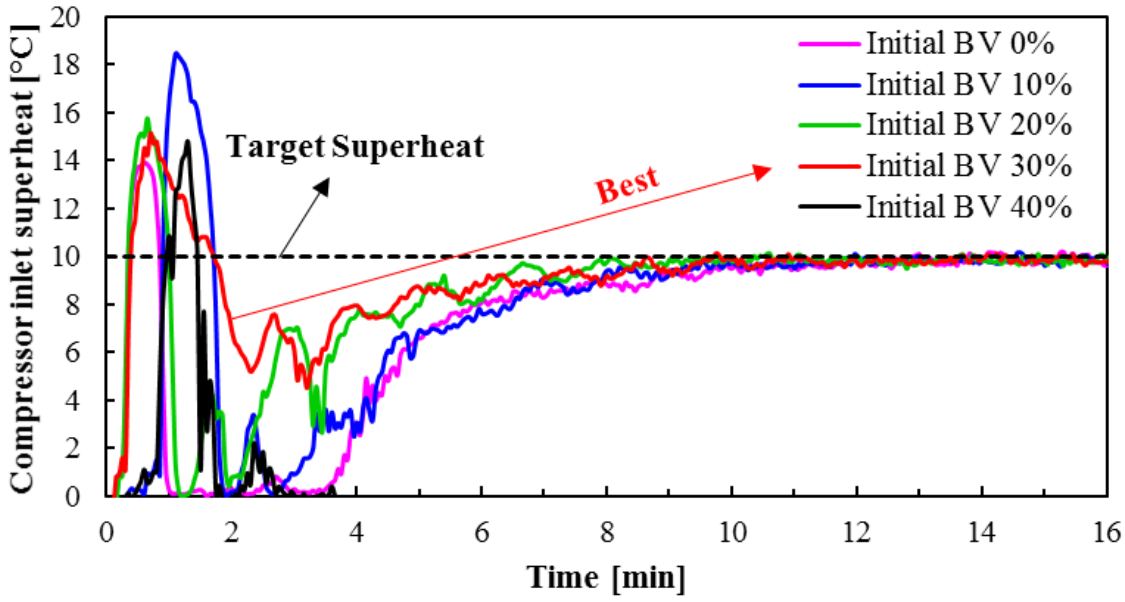


Figure 3-5 Superheat variation under different initial BV opening

Table 3-4 listed the test condition for study in initial BV opening effects. As shown in Figure 3-5, 30% initial opening of bypass valve will be the best choice which prevents liquid coming into compressor during the whole start-up process. When the initial BV

opening is too small, too much liquid will be sent into the evaporator and it took a relatively long time for the BV to accommodate this effect, leading to longer dangerous time for compressor. However, if the initial opening is higher than 40%, the liquid will easily find another path, that is directly from the bypass valve, to flood the compressor. Under the function of PID controller, the valve will be open even more as shown in Figure 3-6 following the basic logic that opening the valve will increase superheat, which is not the case when liquid is going through the bypass valve directly.

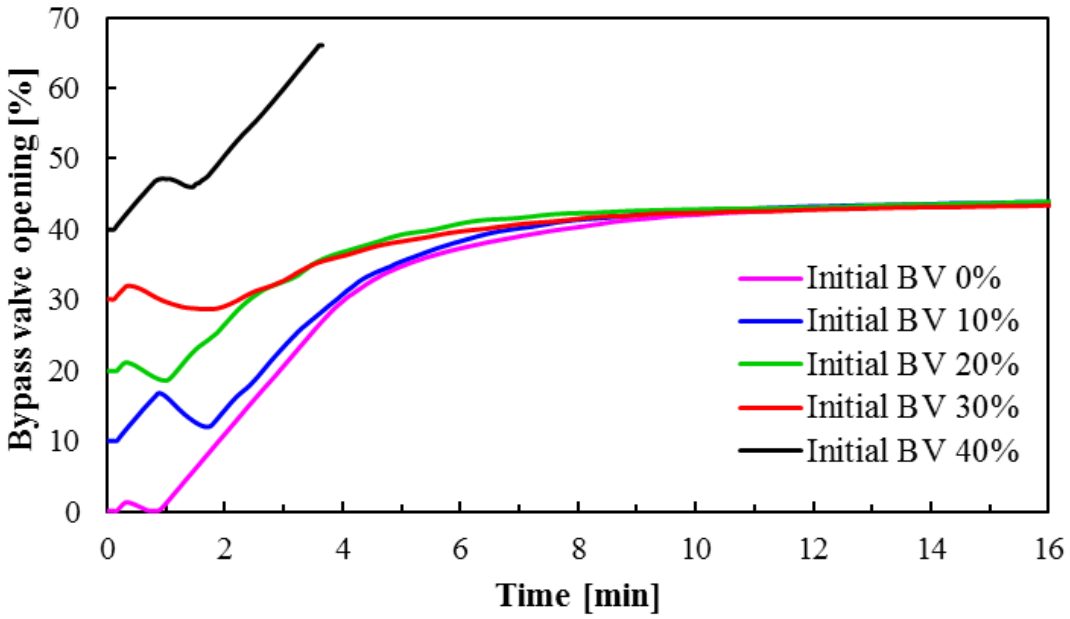


Figure 3-6 Bypass valve opening variation under different initial opening

A more detailed analysis and liquid level variation during start-up under 30% initial BV opening will be discussed in Figure 3-7, where superheat of evaporator outlet and compressor inlet together with liquid level variations with time are plotted.

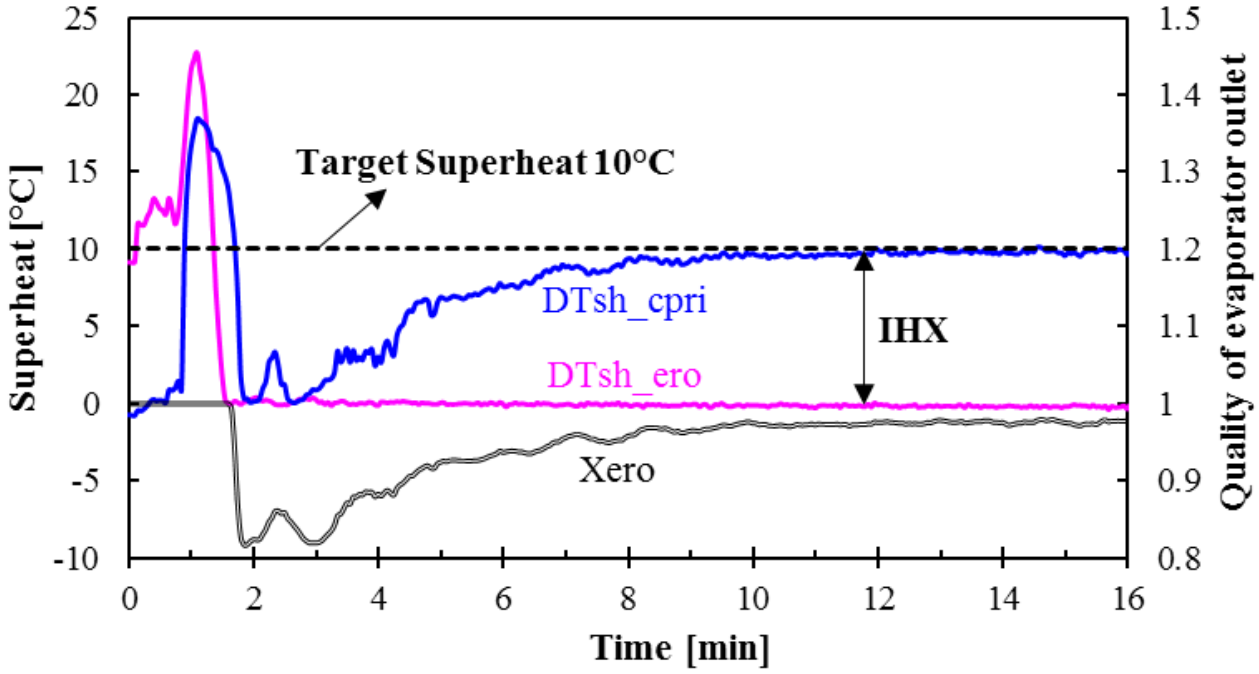


a)

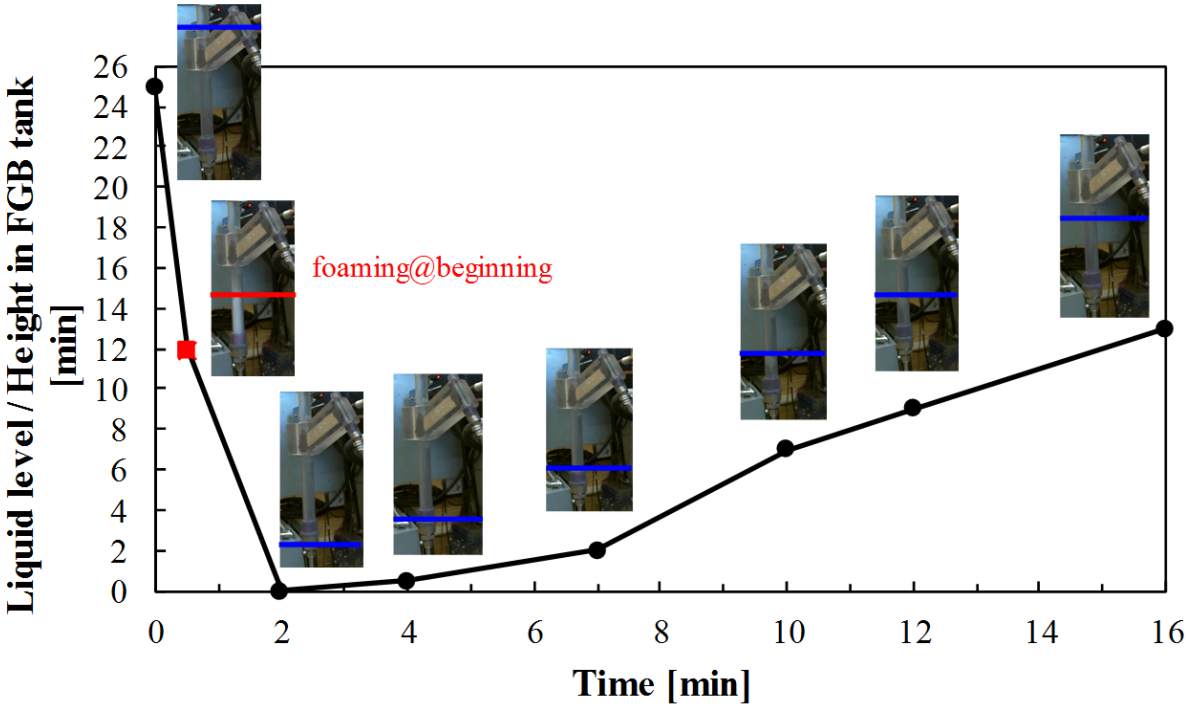


b)

Figure 3-7 Liquid level, quality and superheat of evaporator outlet and superheat of compressor inlet during start-ups: a) superheat and quality variation; b) refrigerant height in FGB tank

At the first minute, refrigerant in the evaporator together with excessive liquid stored in FGB tank quickly evaporate. A clear foaming phenomenon inside FGB tank is shown in the second photo at 30 seconds of Figure 3-7(b). Then from 1 to 4 minute, very low liquid level in FGB tank indicates almost all liquid refrigerant is sent to evaporator, causing the quality from evaporator outlet drops down from 1. Afterward, with the function of PID controller, BV opens more to raise up the liquid level until the superheat of compressor inlet (DTsh_cpri) reach the target 10°C. It should be noted that even though DTsh_cpri reaches 10°C, superheat of evaporator outlet (DTsh_ero) is still around 0 and quality is around 0.98, indicating that two phase is coming out from evaporator outlet. The difference of these two superheat is coming from the internal heat exchanger. This phenomenon is good for system performance, especially good for distribution in evaporator because dry-out region is decreasing dramatically. In conclusion, 30% initial opening is the optimal one recommended for later experiments.

The experimental results clearly show that good control strategy and proper sizing of FGB tank and bypass valve will ensure the safety during start-ups. The actual sizing of valve and tank might be different from system to system since it also depends on the size of heat exchanger, but this study provides a guideline and method to sizing these parameters accordingly.

# CHAPTER 4 FGB SYSTEM IN START-UPS: CONTROL STRATEGY AND EXPERIMENTAL RESULTS

After deciding the proper size of FGB tank and bypass valve, another important thing is the PID controller that are used to control subcooling and superheat automatically. Ideally, the superheat of compressor inlet should always be maintained above zero and the subcooling should reach the optimal valve as soon as possible if the PID controllers function properly, regardless of start-ups or transient system operations. PID parameters should be well chosen and it should work out under different working conditions. This Chapter will focus on the tuning of PID controller and discussed the start-ups under different working conditions. In next Chapter, transients will be discussed using the same PID settings.

## 4.1 PID parameters / PID tuning

PID controller is a control loop feedback mechanism commonly used in industrial control system. It calculated the error value between the desired setpoint and measured process variable and applies a correction based on proportional, integral, and derivative terms. Determination of P, I and D or the so-called PID gains are critical to transient behavior of PID controllers, therefore it's necessary and crucial to finding out a set of appropriate PID gains to reach the optimal performance for the system performance under start-up and transients no matter for which test conditions. Next, the control algorithm and

tuning principle are discussed in details and the user interface is shown to provide a proper way for determination of PID gains.

### 4.1.1 Control algorithm and tuning principle

For subcooling control, the control algorithm is shown in Figure 4-1(a). At condenser outlet (Point 3 in Figure 2-2), sensors including pressure transducer and thermocouple are used to measure actual pressure (Pcro) and temperature (Tcro) and the in-time subcooling (DTsc_cro) is obtained by computation. The difference between setup subcooling and actual measured value serves as input error signal for PID controller. And the controller attempts to minimize the error over time by adjustment of a control variable, which is the opening of expansion valve. The same logic goes for superheat control except that the process variable, or in-time superheat, is measured by pressure transducer and thermocouple of compressor inlet (Pcpri and Tcpri).

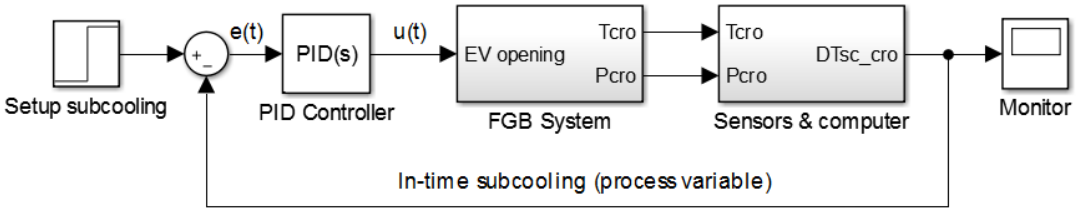


(a)

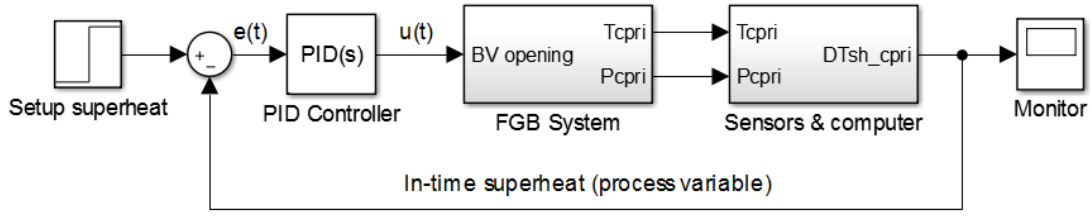


(b)

Figure 4-1 Control algorithm (a) subcooling control; (b) superheat control

By choosing appropriate $K_p$, $K_i$, $K_d$ (also denotes as P, I and D), the two controllers can help the FGB system quickly achieve the desired subcooling and superheat, therefore make the system quickly transits to steady state. The algorithm of PID controller is shown in Equation (4-1).

$$u(t) = K_p e(t) + K_i \int_0^t \tau(t) d\tau + K_d \frac{d}{dt} e(t) \quad (4\text{-}1)$$

where e is the error by the difference between set point and process variable, t is the instantaneous time, $\tau$ is the variable of integration which takes the value from time 0 to present time t. $K_p$ (P), the proportional gain, accounts for present value of error, therefore the control output will be large and positive if the error is large and positive. $K_i$ (I), the integral gain, accounts for past value of error, and the controller will have stronger action if the integral of the error accumulates over time. $K_d$ (D), the derivative gain, accounts for possible future trends of the error. Since the sampling time is 3 seconds which is not continuous and the air-conditioning system is a large time-delay system, using I value will easily cause very big overshoot and make the system unstable. So, we only use PD controller in the experiments. After trial and fail, finally, we found a relative better PID parameter combinations under 25°C ambient temperature as shown in Table 4-1, which is also the parameters we used in Chapter 3.

Table 4-1 PID parameters

| | **P** | **I** | **D** |
|---|---|---|---|
| Subcooling control | 0.3 | 0 | 0.1 |
| Superheat control | 0.05 | 0 | 0 |

## 4.1.2 Automatic testing user interface

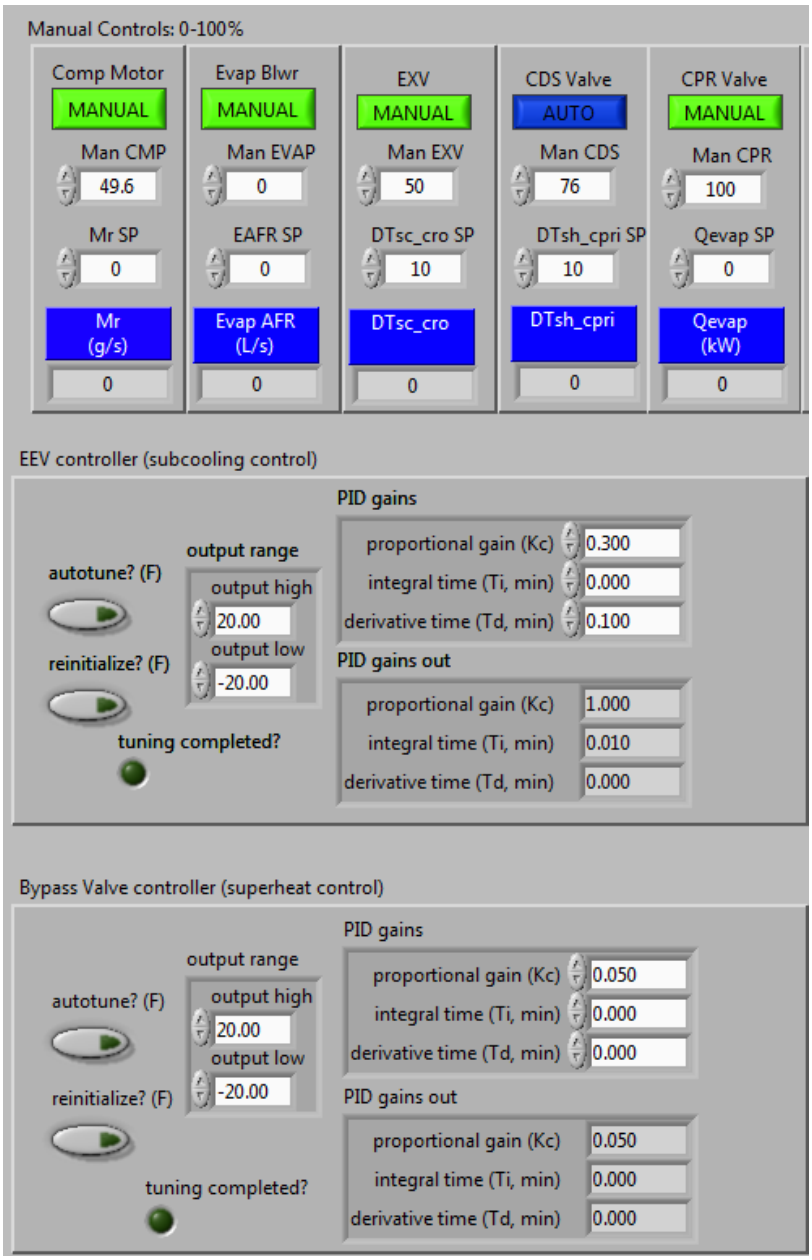


Figure 4-2 User interface for subcooling and superheat controller

The subcooling control and superheat control was programmed in data acquisition software LabVIEW where the built-in control module was used to control the EV and BV. The user interface of the subcooling and superheat controller is shown in Figure 4-2. It gives two options to control opening of valves, manually and automatically. In auto mode, the PID controller will automatically control the opening of EV and BV, making

subcooling and superheat reach the set point as soon as possible. In manual mode, the opening can be keyed in manually to control subcooling and superheat. In the experiment, once we turn on the compressor, nothing need to be changed manually and the system will work automatically including valves opening, air flow rate, etc.

## 4.2 Verification of PID parameters at different working conditions

For different working conditions, the optimal set of PID combination will be different. But for industrial application, it is much easier to use the same PID values and make the system stabilize for a wide range of working conditions. To demonstrate the robustness of the control strategy, start-up tests for four different working loads are performed under the test conditions shown in Table 3-3. It should be noted that the indoor and outdoor chamber temperature which are controlled by electrical heaters and condensing is kept within 1°C of the desired temperature. PID parameters for subcooling and superheat controller are set as shown in Table 4-1. The PID controllers are turned on once the compressor starts working so the system will work automatically. The subcooling and superheat variations shown in Figure 4-3 demonstrate good performance during start-ups. Subcooling will reach the desired value within 5 minutes and no liquid will be flooding the compressor since the superheat is always kept above 3°C, indicating safe starts for all working conditions. Figure 4-4 shows the P-h diagram under steady state for different working conditions where we can clearly find that by increasing the chamber temperature, P-h diagram will shift up due to higher working loads.

Even though the PID parameters would be different from system to system, this study gives a guideline and example of FGB system start-ups under automatic control.

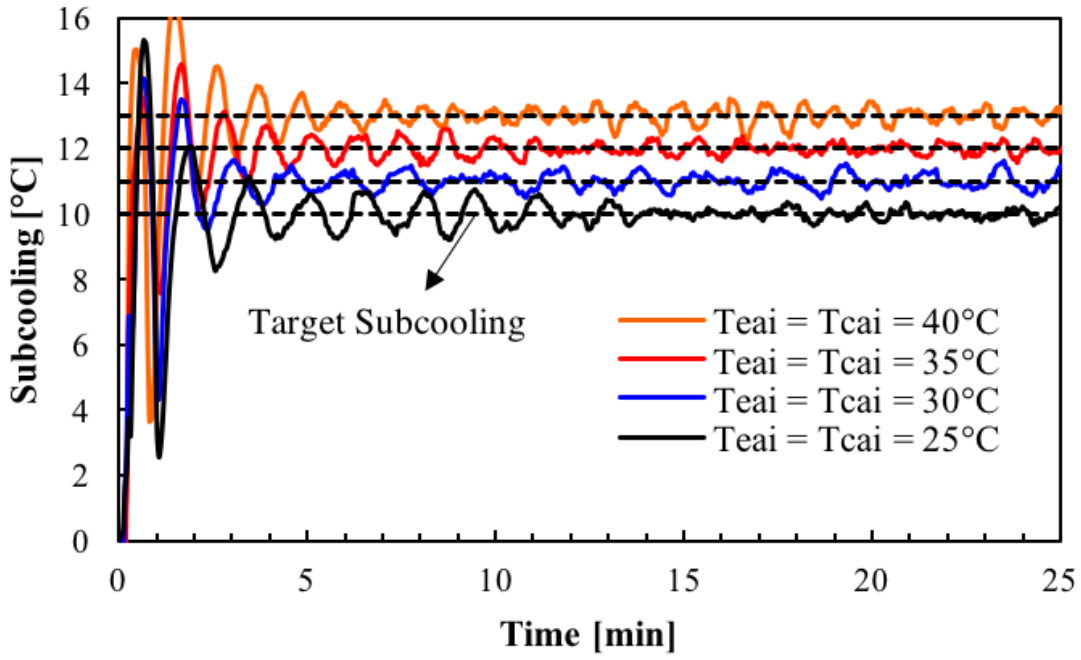


(a)

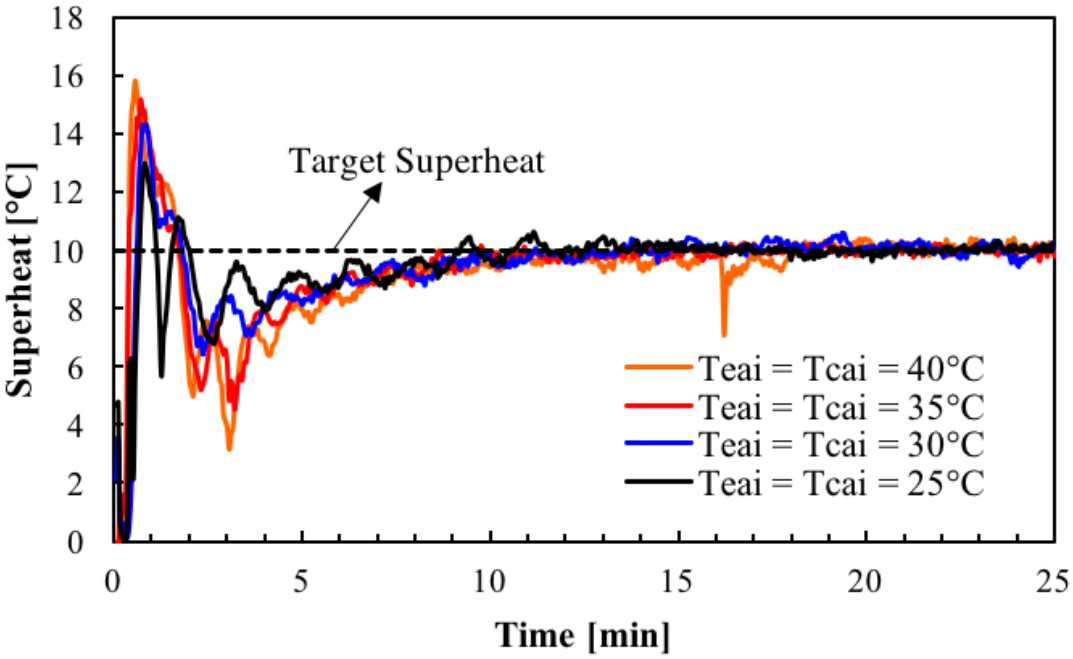


(b)

Figure 4-3 Subcooling and superheat variations at start-up under different

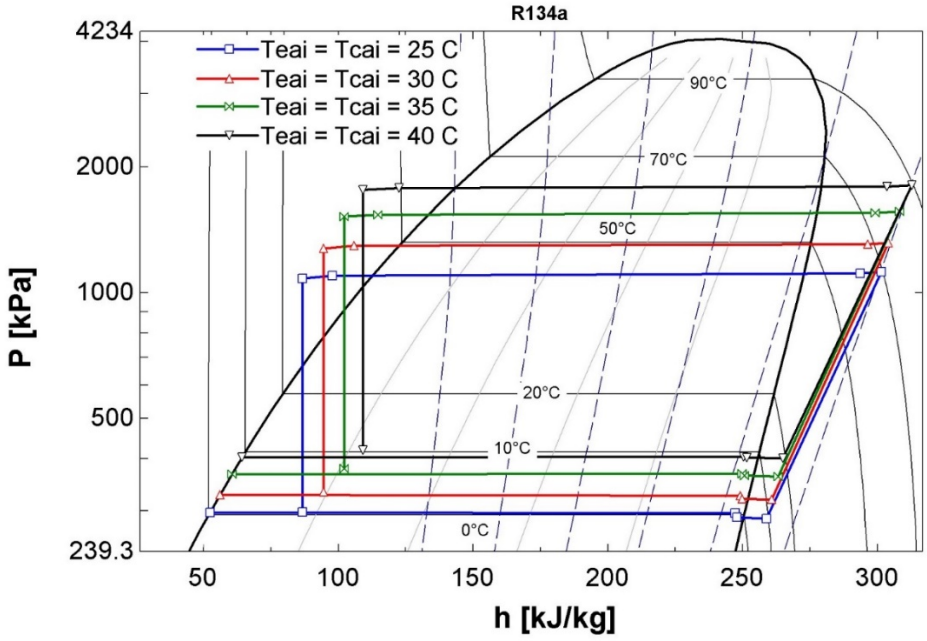


Figure 4-4 P-h diagram for different chamber temperatures

# CHAPTER 5 EXPERIMENTAL VERIFICATION OF SYSTEM ROBUSTNESS IN TRANSIENTS

After investigating start-ups for FGB system, it is also interesting to know how the system will behave under transients under step changes such as air mass flow rate of indoor heat exchanger, face velocity of outdoor exchanger and compressor speed. To demonstrate the system robustness, the same PID parameters as Chapter 3 and 4 are used in the tests below. At 10 minute, step change is made and the system would transfer from one steady state to another one with automatically control.

## 5.1 System response to step change of air mass flow rate of evaporator

The first scenario is changing air mass flow rate. After 10 minutes' steady state, the air mass flow rate for evaporator will be decreased from 9kg/min to 6.5 kg/min. As a result of the step change, the heat transfer coefficient on the evaporator air side decreases, causing the LMTD of evaporator side increases. Therefore, the evaporator side pressure, which is normally denoted as low pressure of the refrigeration cycle, will decrease as Figure 5-1 shown. The same phenomenon can also be presented by P-h diagram shown in Figure 5-2.

Table 5-1 Test conditions for step function change in air mass flow rate of evaporator

| Change | Compressor Speed (rpm) | Condenser | | Evaporator | |
|---|---|---|---|---|---|
| | | Temp (°C) | Face Velocity(m/s) | Temp (°C) | Mass Flow (kg/min) |
| Before | 900 | 35 | 1.5 | 35 | **9** |
| After | 900 | 35 | 1.5 | 35 | **6.5** |

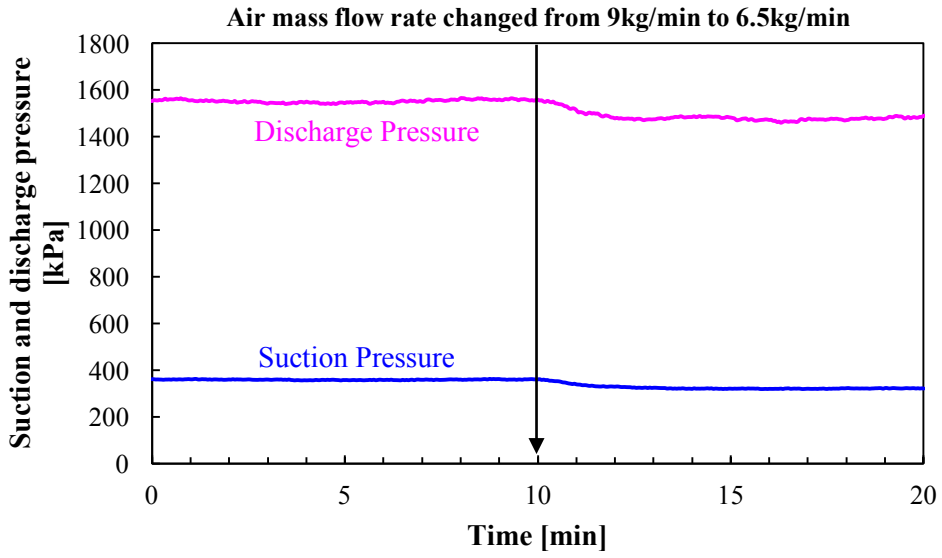


Figure 5-1 Pressure variations during transients of change in air mass flow rate of evaporator

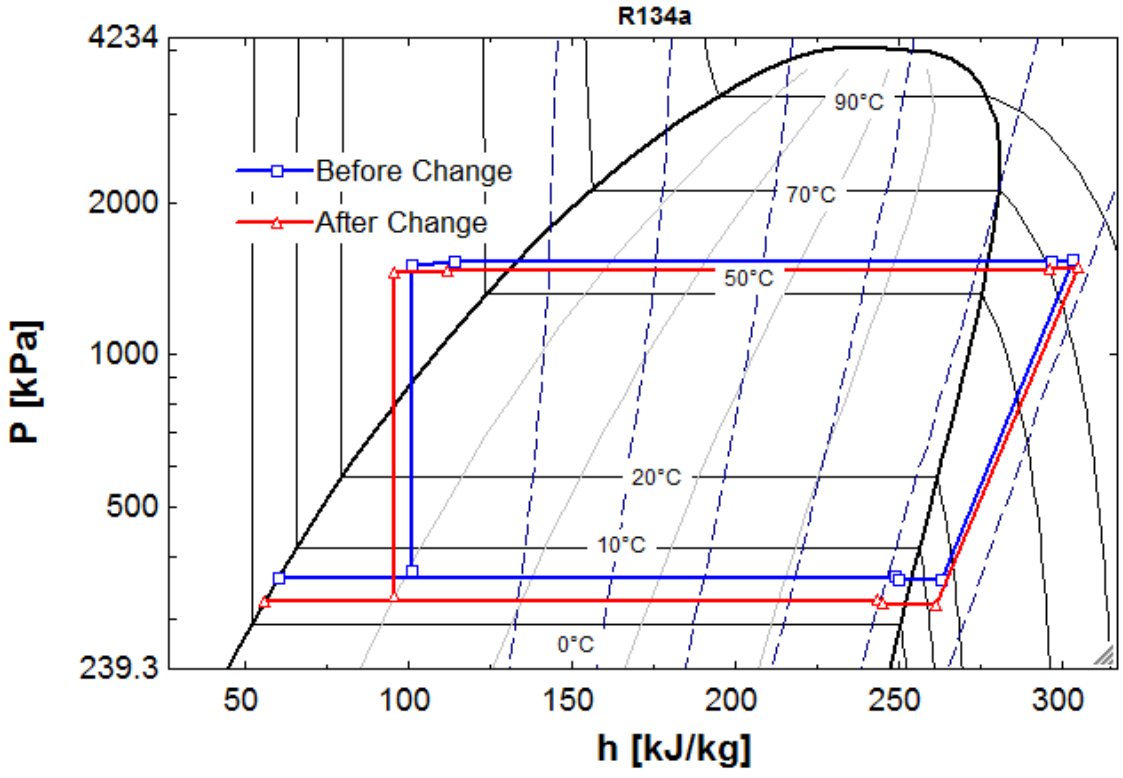


Figure 5-2 P-h diagram before and after change of air mass flow rate of evaporator

As shown in Figure 5-3 and Figure 5-4, the subcooling and superheat will be stable within 3 minutes under automatic adjusting of the valves. Since the mass flow rate change is not very big, the change before and after change is not obvious.

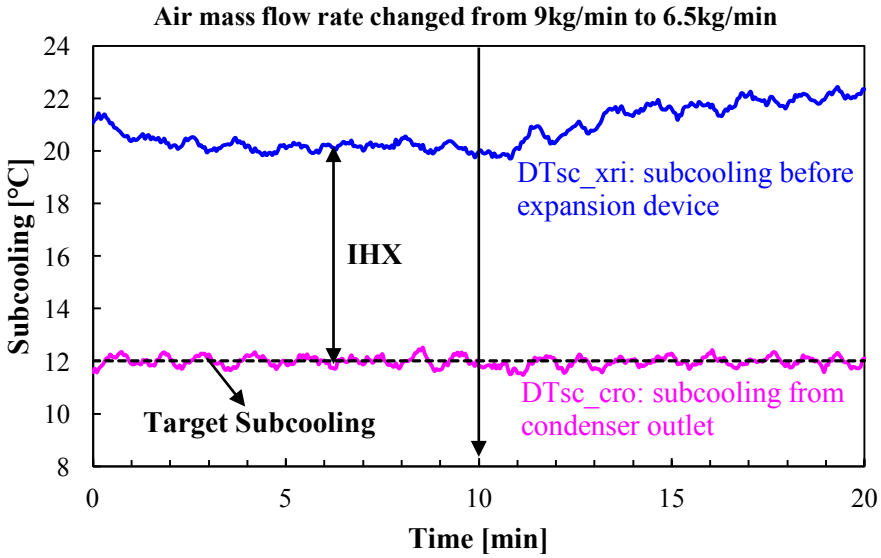


Figure 5-3 Subcooling variations during transients of change in air mass flow rate of evaporator

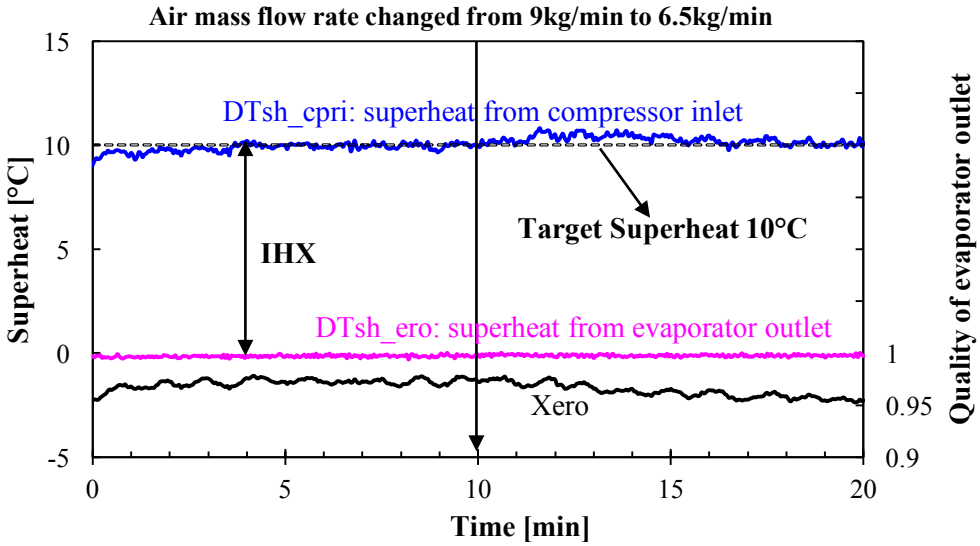


Figure 5-4 Superheat variations during transients of change in air mass flow rate of evaporator

## 5.2 System response to step change of air face velocity of condenser

The second scenario is changing air face velocity. After 10 minutes' steady state, the air face velocity for condenser will be increased from 1.5 m/s to 3m/s. The priciple is similar to the step change of air mass flow rate of evaporator where in this case the heat transfer coefficient on the condenser air side increases causing the LMTD of condenser side decreases. That is why the condenser side pressure will decrease as Figure 5-5 shown. The same phenomenon can also be presented by P-h diagram shown in Figure 5-6.

Table 5-2 Test conditions for step function change in air face velocity of condenser

| Change | Compressor Speed (rpm) | Condenser | | Evaporator | |
|---|---|---|---|---|---|
| | | Temp (°C) | Face Velocity(m/s) | Temp (°C) | Mass Flow (kg/min) |
| Before | 900 | 35 | **1.5** | 35 | 9 |
| After | 900 | 35 | **3.0** | 35 | 9 |

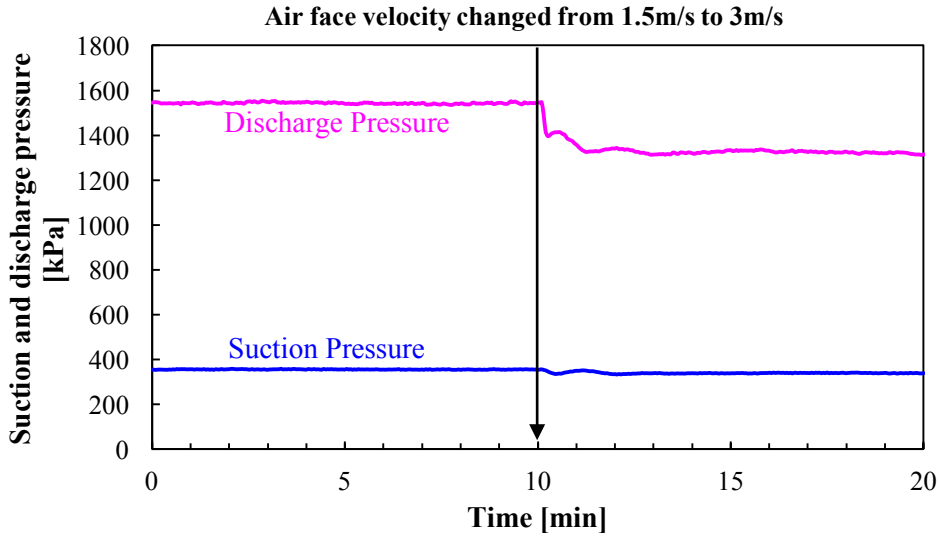


Figure 5-5 Pressure variations during transients of change in air face velocity of condenser

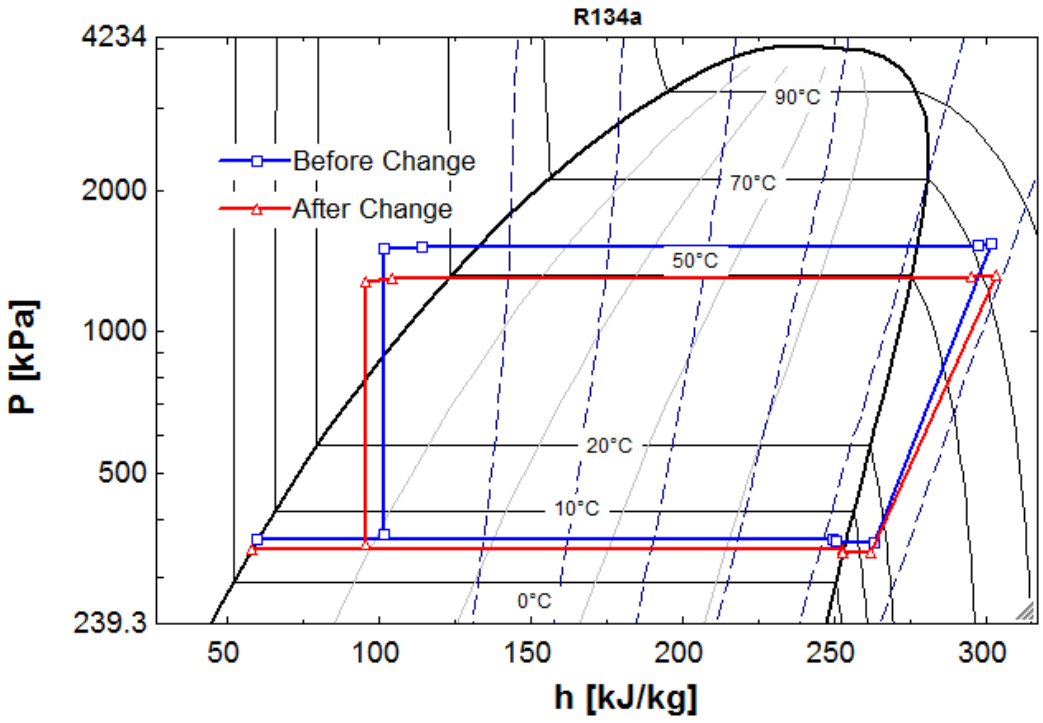


Figure 5-6 P-h diagram before and after change of air face velocity of condenser

As shown in Figure 5-7 and Figure 5-8, the subcooling and superheat will also be stable after 4 minutes' automatic adjusting of the valves.

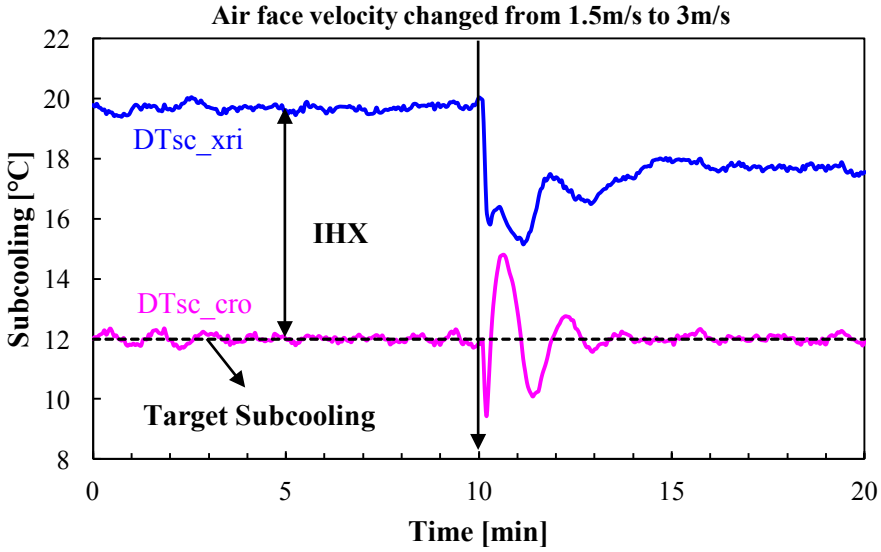


Figure 5-7 Subcooling variations during transients of change in air face velocity of condenser

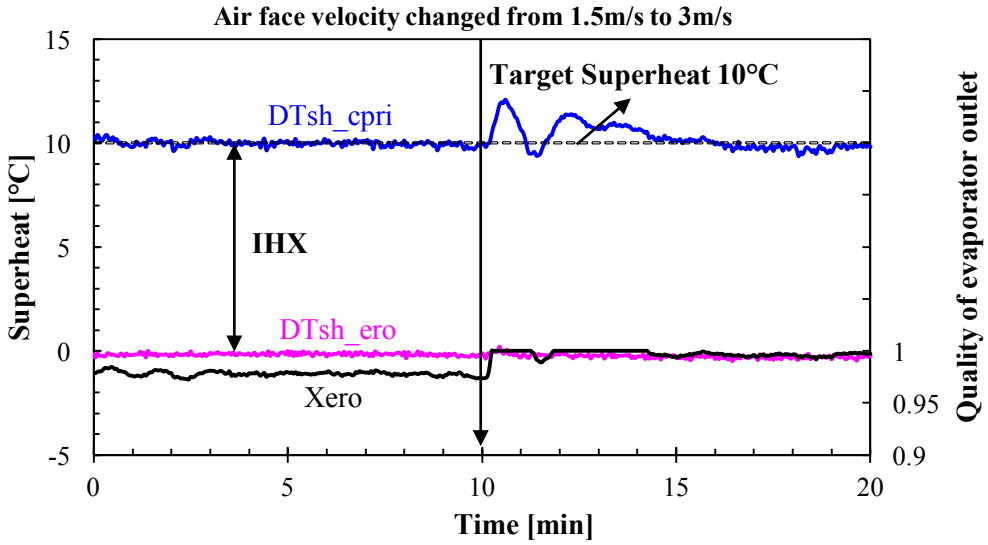


Figure 5-8 Superheat variations during transients of change in air face velocity of condenser

## 5.3 System response to step change of compressor speed

The third scenario is changing compressor speed from 900 to 1200 rpm. After 10 minutes' steady state, the compressor speed will be increased. Therefore the mass flow rate will increase causing the LMTD of both evaporator and condenser side increases. That is why the condenser side pressure will increase and the evaporator side pressure will decrease as shown in Figure 5-9. The same phenomenon can also be presented by P-h diagram shown in Figure 5-10.

Table 5-3 Test conditions for step function change in compressor speed

| Change | Compressor Speed (rpm) | Condenser | | Evaporator | |
|---|---|---|---|---|---|
| | | Temp (°C) | Face Velocity(m/s) | Temp (°C) | Mass Flow (kg/min) |
| Before | **900** | 35 | 1.5 | 35 | 9 |
| After | **1200** | 35 | 1.5 | 35 | 9 |

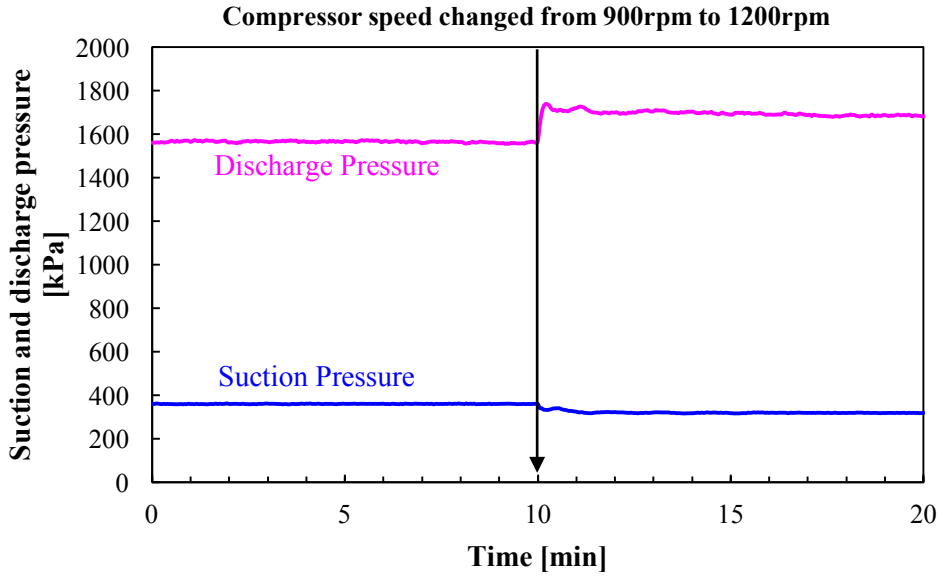


Figure 5-9 Pressure variations during transients of change in compressor speed

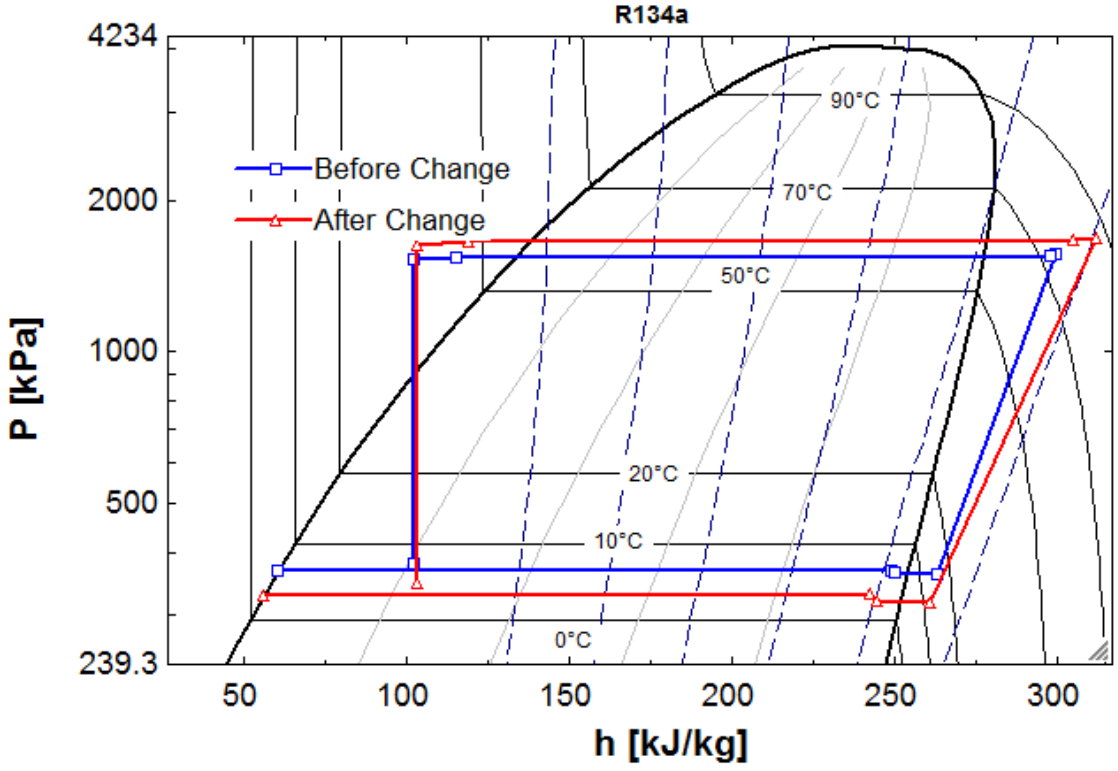


Figure 5-10 P-h diagram before and after change of compressor speed

As shown in Figure 5-11 and Figure 5-12, the moment compressor speed increase, more liquid is sent to evaporator. As a result, the quality of evaporator outlet will decrease meaning that more liquid will be sent to the internal heat exchanger so the superheat will drop a little bit as first. Finally, subcooling and superheat will also be stable after 3 minutes' automatic adjusting of the valves.

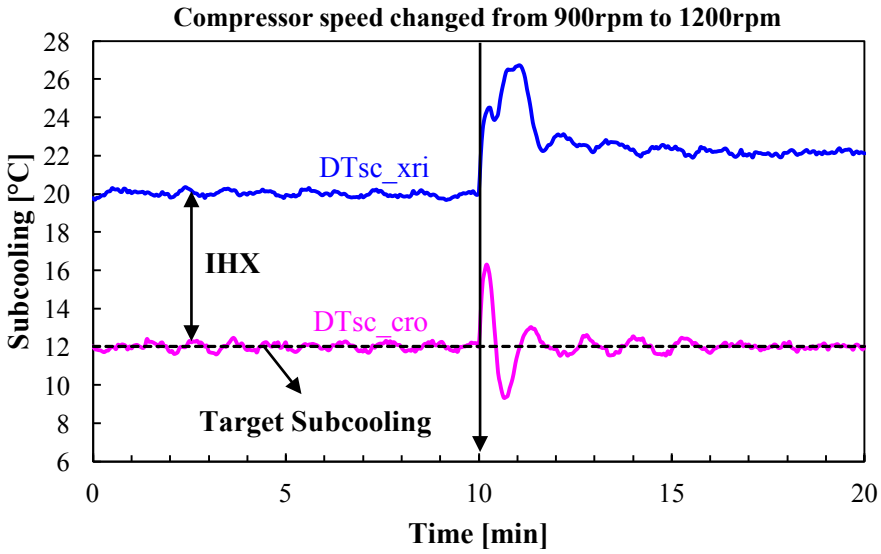


Figure 5-11 Subcooling variations during transients of change in compressor speed

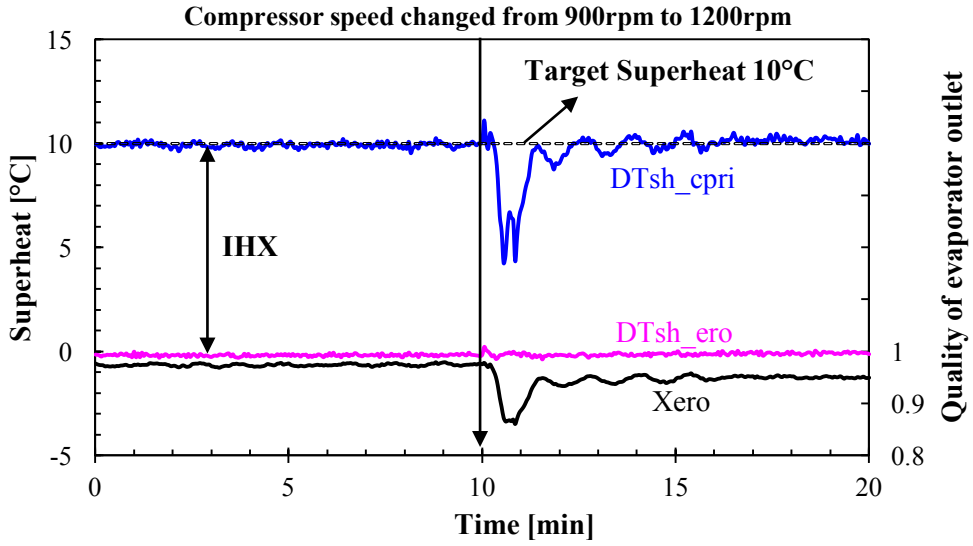


Figure 5-12 Superheat variations during transients of change in compressor speed

## 5.4 Discussion

Based on the step change in air mass flow rate for evaporator, air face velocity for condenser and compressor speed, the control strategy for FGB is demonstrated to be stable and system robustness is proven. When changes are taken, the system will react to this change and the cycle will move accordingly. Nevertheless, under the function subcooling and superheat controller, system will correct the opening of EV and BV thus creating a new steady state.

# CHAPTER 6 CONCLUSION

This study investigates the experimental control strategy of flash gas bypass system, mainly for automobile air condition. Start-up and transient performance have been studied to make sure system can be well-functioned and robust. In the experiments, an EV coupled with a PID controller in data acquisition software was implemented to provide in-time and accurate control of the subcooling from condenser outlet which is proven to be an additional beneficial way to increase the system performance. To ensure no liquid would come into compressor, an BV coupled with another PID controller was also implemented to provide accurate control of superheat from compressor inlet. In the study of start-ups, size of bypass valve and size of FGB tank were investigated to make sure that the components are well-chosen. The initial opening of bypass valve is also studied in details to prevent flooded compressor and a thoroughly explanation between liquid level and superheat was provided. It was found that for this system, 30% would be the better initial opening of BV to avoid liquid in compressor suction during start-ups. Through the experiments for different working conditions, the chosen PID parameters could provide accurate control of the EV and BV to reach the target subcooling and superheat. Finally, to verify the system robustness, three step changes including air mass flow rate of evaporator, air face velocity of condenser and compressor speed was performed and the system exhibits good control ability to maintain the target subcooling and superheat.

# REFERENCES


Beaver, A.C., Yin, J., Bullard, C.W., Hrnjak, P.S., 1999. An Experimental Investigation of Transcritical Carbon Dioxide Systems for Residential Air-Conditioning. ACRC Report CR-18. University of Illinois at Urbana-Champaign.

Elbel, S. and Hrnjak, P., 2004. Flash gas bypass for improving the performance of transcritical R744 systems that use microchannel evaporators. *International Journal of Refrigeration*, 27(7), pp.724-735.

Kim, N.H., Kim, D.Y. and Byun, H.W., 2011. Effect of inlet configuration on the refrigerant distribution in a parallel flow minichannel heat exchanger. *International journal of refrigeration*, *34*(5), pp.1209-1221.

Kulkarni, T., Bullard, C.W. and Cho, K., 2004. Header design tradeoffs in microchannel evaporators. *Applied Thermal Engineering*, *24*(5), pp.759-776.

Li, H. and Hrnjak, P., 2015a. An experimentally validated model for microchannel heat exchanger incorporating lubricant effect. International journal of refrigeration, 59, pp.259-268.

Li, H. and Hrnjak, P., 2015b. Quantification of liquid refrigerant distribution in parallel flow microchannel heat exchanger using infrared thermography. *Applied Thermal Engineering*, *78*, pp.410-418.

Li, H. and Hrnjak, P., 2016. Visualization and Analysis of Periodic Reverse Flow in an Automobile Microchannel Evaporator (No. 2016-01-0252). SAE Technical Paper.

Li, H. and Hrnjak, P., 2017. Modeling of bubble dynamics in single diabatic microchannel. *International Journal of Heat and Mass Transfer*, *107*, pp.96-104.

Milosevic, A.S., Hrnjak, P.S., 2010. Flash Gas Bypass Concept Utilizing Low Pressure Refrigerants. ACRC Report TR-283. University of Illinois at Urbana-Champaign.

Pottker, G. and Hrnjak, P., 2015. Effect of the condenser subcooling on the performance of vapor compression systems. *International Journal of Refrigeration*, 50, pp.156-164.

Pottker, G. and Hrnjak, P., 2015. Experimental investigation of the effect of condenser subcooling in R134a and R1234yf air-conditioning systems with and without internal heat exchanger. *International Journal of Refrigeration*, 50, pp.104-113.

SAE Standard J2765_200810, 2011. Procedure for Measuring System COP [Coefficient of Performance] of a Mobile Air Conditioning System on a Test Bench.

Tuo, H., Bielskus, A. and Hrnjak, P., 2011. Effect of flash gas bypass on the performance of R134a mobile air-conditioning system with microchannel evaporator. *SAE International Journal of Materials and Manufacturing*, 4(2011-01-0139), pp.231-239.

Tuo, H., Hrnjak, P.S., 2012a. Experimental Study of Refrigerant Two Phase Separation in Compact Vertical T-junction. *ASHRAE 2012 Winter Conference*, Paper. CH-12-C086.

Tuo, H., Hrnjak, P.S., 2012b. An Experimentally Validated Model of Refrigerant Distribution in a Parallel Microchannel Evaporator. *SAE 2012 Congress*, Paper. 2012-01-321.

Tuo, H. and Hrnjak, P., 2012. Flash gas bypass in mobile air conditioning system with R134a. *International journal of refrigeration*, 35(7), pp.1869-1877.

Tuo, H. and Hrnjak, P., 2013. Periodical reverse flow and boiling fluctuations in a microchannel evaporator of an air-conditioning system. *International journal of refrigeration*, *36*(4), pp.1263-1275.

Tuo, H. and Hrnjak, P., 2014. Visualization and measurement of periodic reverse flow and boiling fluctuations in a microchannel evaporator of an air-conditioning system. *International Journal of Heat and Mass Transfer*, *71*, pp.639-652.

Tuo, H. and Hrnjak, P., 2014. Vapor–liquid separation in a vertical impact T-junction for vapor compression systems with flash gas bypass. International journal of refrigeration, 40, pp.189-200.

Vist, S. and Pettersen, J., 2004. Two-phase flow distribution in compact heat exchanger manifolds. *Experimental thermal and fluid science*, *28*(2), pp.209-215.

Xu, L. and Hrnjak, P.S., 2014. Potential of Controlling Subcooling In Residential A/C System. ACRC Report TR-311. University of Illinois at Urbana-Champaign.

Zou, Y., Hrnjak, P. S., 2013, Experiment and visualization on R134a upward flow in the vertical header of microchannel heat exchanger and its effect on distribution, *International Journal of Heat and Mass Transfer*, 62,124-134.

Zou, Y. and Li, H., 2014. R134a and PAG Oil Maldistribution and Its Impact on Microchannel Heat Exchanger Performance. *ASHRAE Transactions*, *120*, p.J1.

# APPENDIX A. COMPONENTS OF TEST FACILITY

In Appendix A, a more detailed description of the components used in this study will be presented.

One of the most important component is FGB tank shown in Figure A-1. A more detailed study of the geometry and the separation efficiency can be found in paper from Tuo and Hrnjak (2014). The FGB tank was manufactured to be transparent to record liquid level.

Figure A-1 FGB tank

A Sporlan model SER-A EEV is used as expansion devices and a picture is shown in Figure A-2. The Sporlan IB Series Interface Boards are used together with the data logger to enable the automatic control of its opening. The opening of EEV from 0 to 100% will be actuated by 0-10 V input signal to the IB board. The voltage will be adjusted by the computer through the data logger.

Figure A-2 Electronic expansion valve (from the internet)

The photo of the microchannel evaporator is shown in Figure A-3. The overall dimensions for this evaporator is 12 inches by 9.25 inches. The fin density is about 0.78 fin/mm and the inlet and outlet headers is about 2 inches' height. It is a single pass evaporator modified from an original Behr 6-pass evaporator for a better distribution.

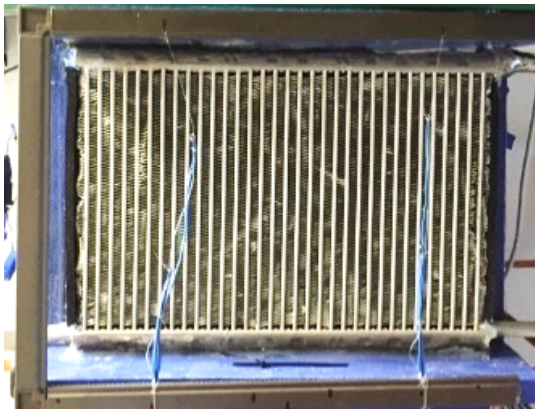

Figure A-3 Microchannel evaporator

The photo of the microchannel evaporator is shown in Figure A-3. The overall dimensions for this evaporator is 12 inches by 9.25 inches. The fin density is about 0.78

fin/mm and the inlet and outlet headers is about 2 inches' height. It is a single pass evaporator modified from an original Behr 6-pass evaporator for a better distribution. The photo of the microchannel 3-pass condenser is shown in Figure A-4. The length is 26.5 inches and width is 13.38 inches.

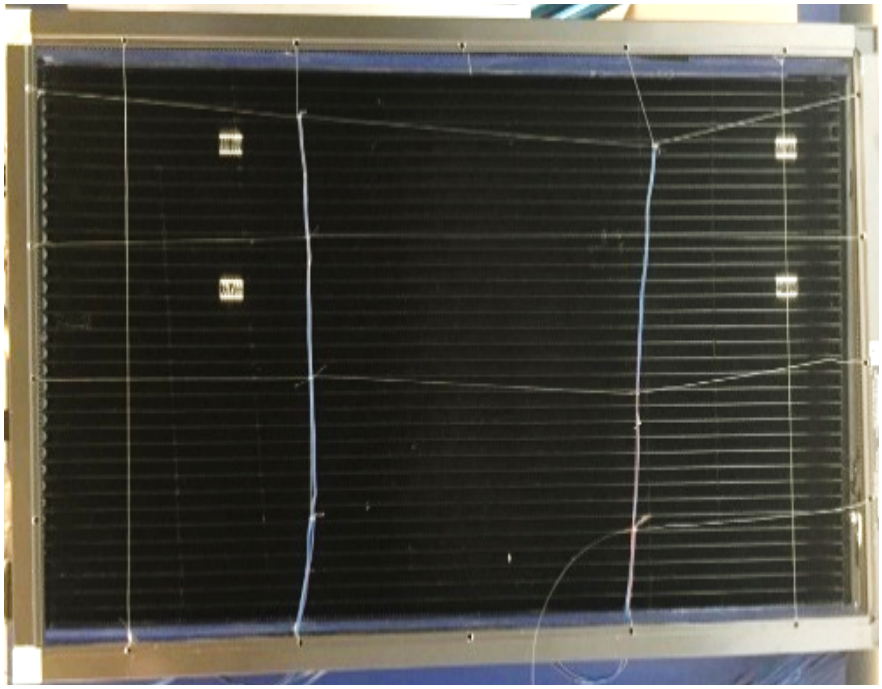

Figure A-4 Microchannel condenser

# APPENDIX B. FACILITY SCHEMATIC

The system is built as a reversible system which can be used as both air conditioner and heat pump. The schematic for each mode is shown in Figure B-1 and Figure B-2. Each component is in the same position for both AC and HP mode. Two sets of 4-way valves are used to transfer between one mode and the other. In AC mode, the indoor heat exchanger will be evaporator and refrigerant from the outlet of the evaporator will go through the internal heat exchanger into compressor. However, in HP mode, the indoor heat exchanger will be condenser and the refrigerant from the outlet of the evaporator will go to expansion device through internal heat exchanger.

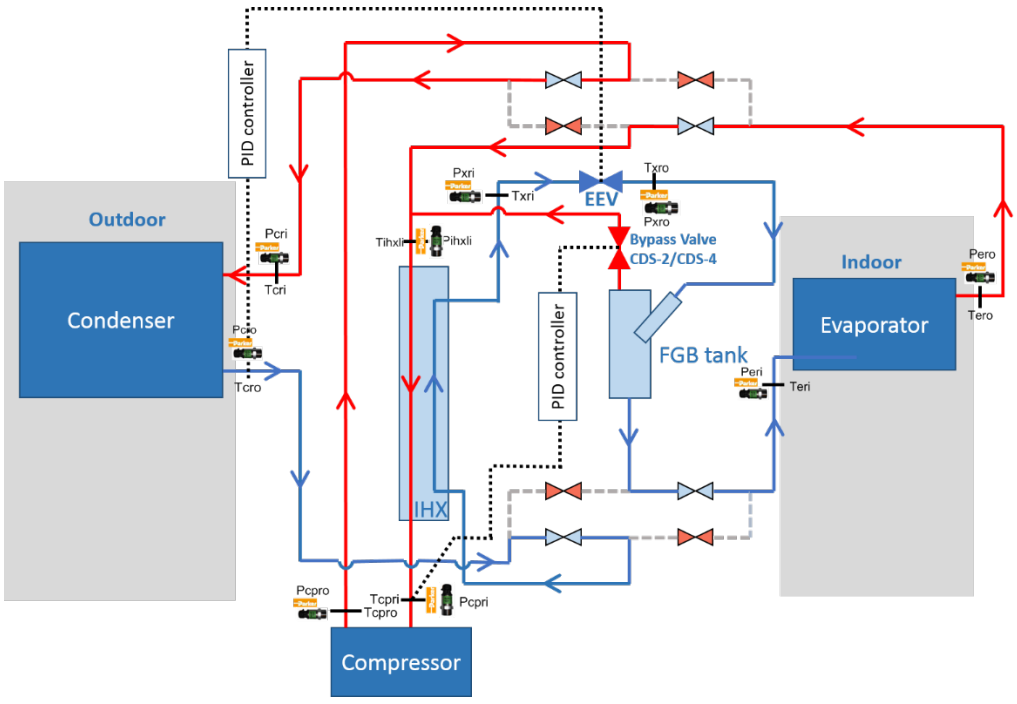


Figure B-1 System schematic for AC mode

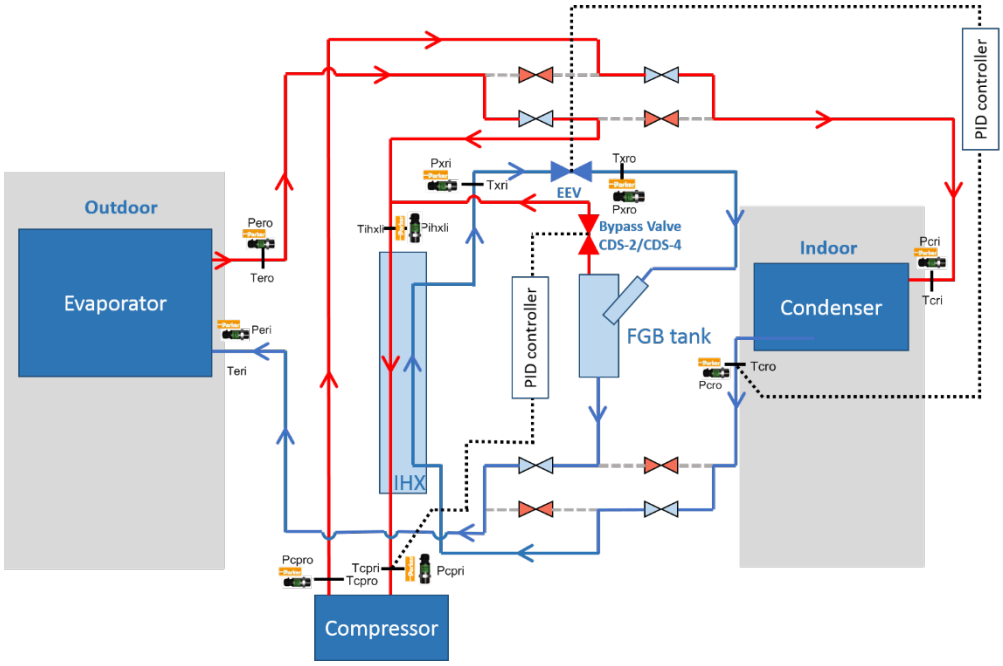


Figure B-2 System schematic for HP mode

# APPENDIX C. TEST RESULTS

In Appendix C, more tests data and figures in transients are shown as backup material.

1. Transients of change in air mass flow rate of evaporator (MFR)

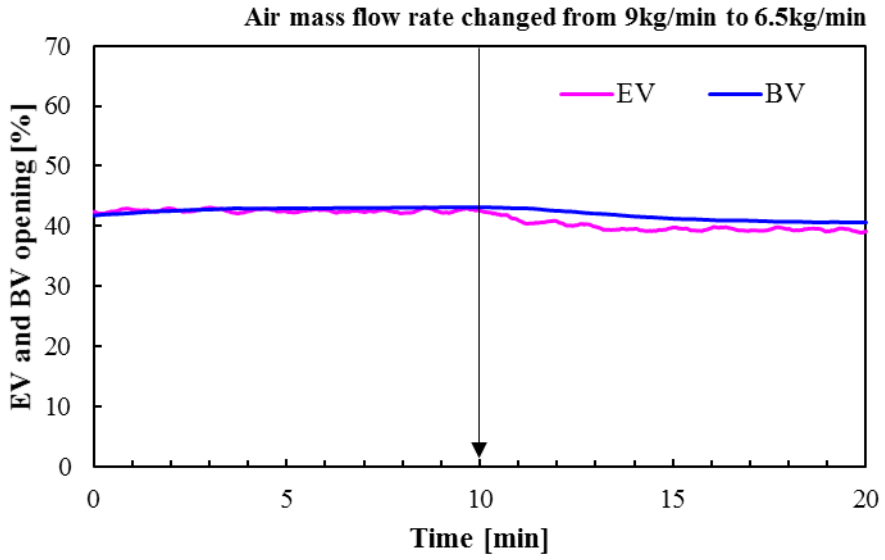


Figure C-1 EV and BV opening variations during transients of change in MFR

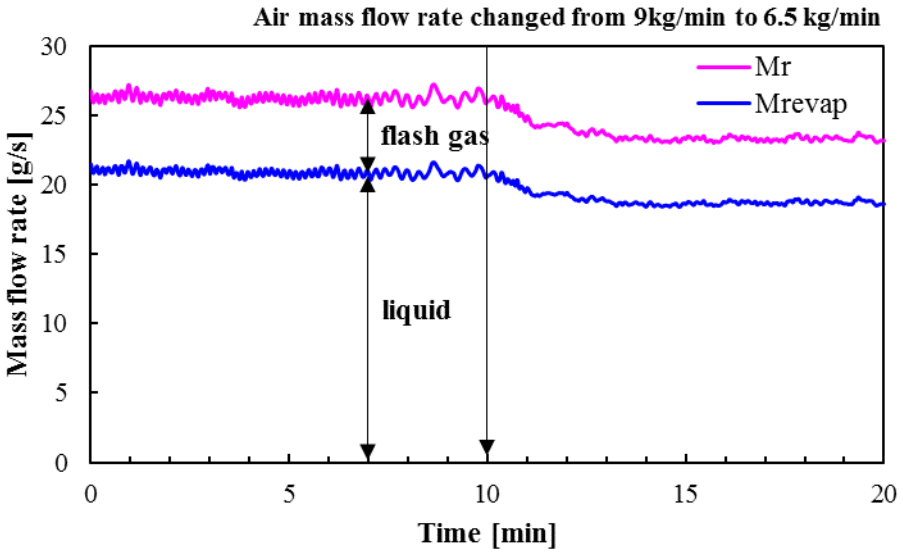


Figure C-2 Mass flow rate variations during transients of change in MFR

2. Transients of change in air face velocity of evaporator (FV)

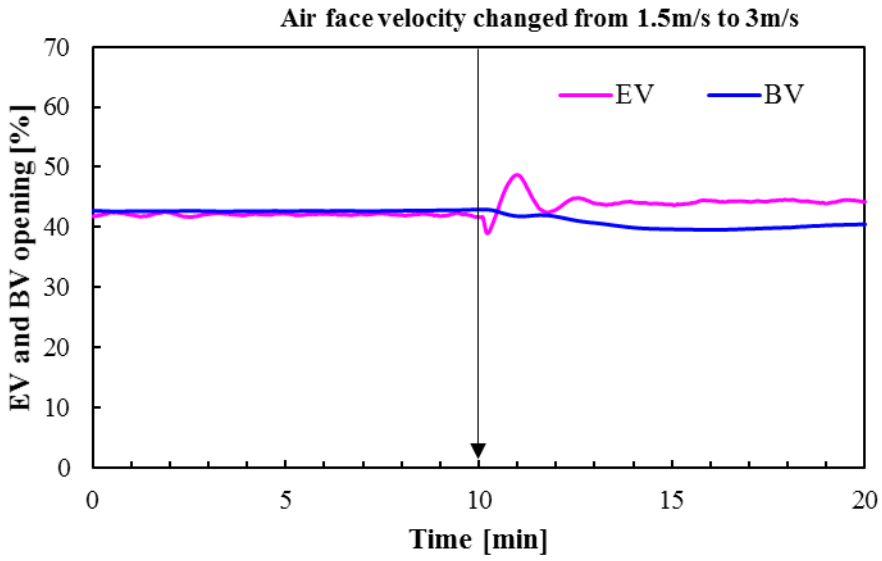


Figure C-3 EV and BV opening variations during transients of change in FV

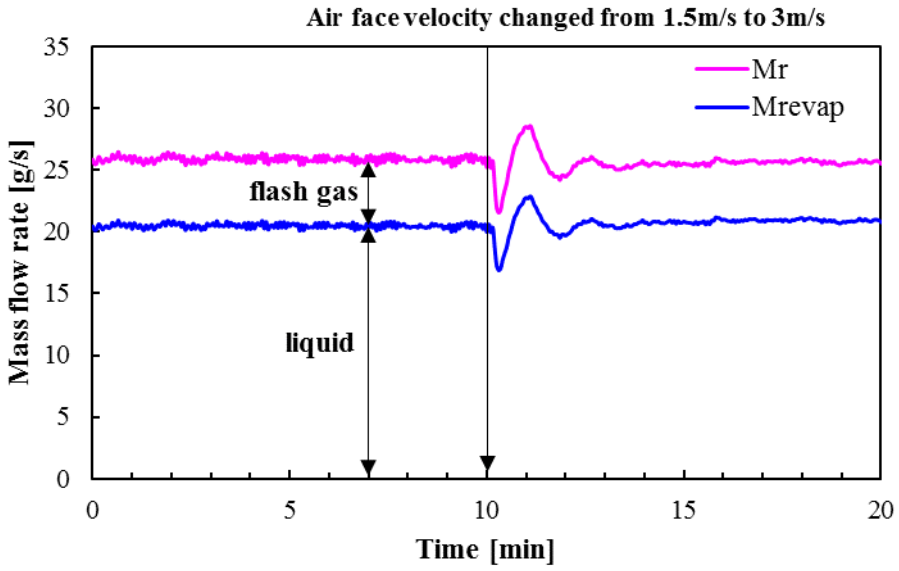


Figure C-4 Mass flow rate variations during transients of change in FV

3. Transients of change in compressor speed

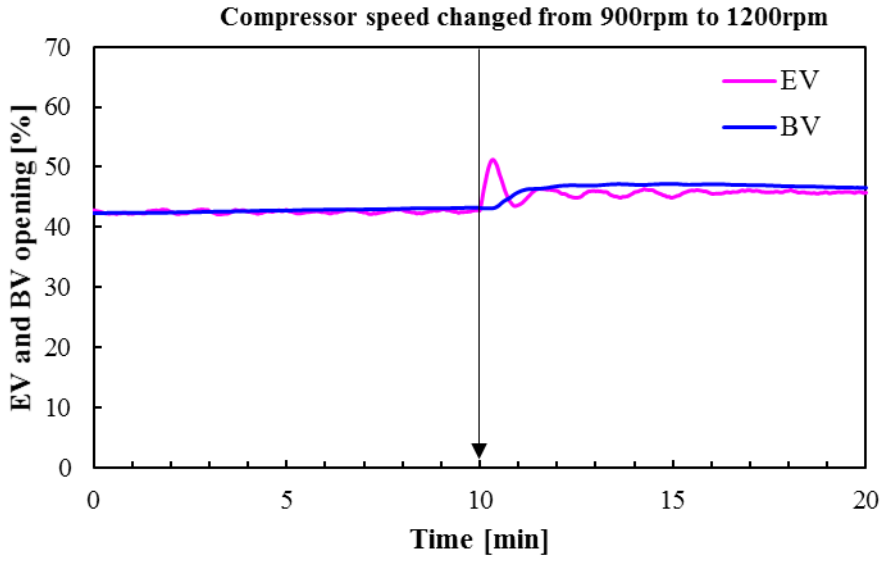


Figure C-5 EV and BV opening variations during transients of change in compressor speed

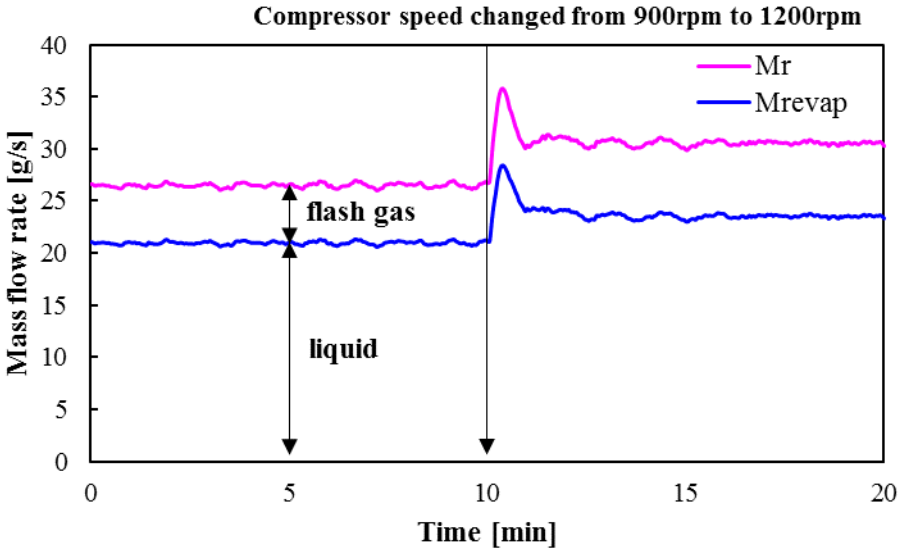


Figure C-6 Mass flow rate variations during transients of change in compressor speed